NTNU – Trondheim
Norwegian University of
Science and Technology

Geological Development of the Jan Mayen Micro Continent and its Continental Margins

Lars Jørgensen Tveito

Petroleum Geoscience and Engineering
Submission date: June 2013
Supervisor: Ståle Emil Johansen, IPT

Norwegian University of Science and Technology
Department of Petroleum Engineering and Applied Geophysics

Abstract

The Jan Mayen micro continent is isolated from other continental crust central in the North Atlantic. This master thesis is a seismic interpretation study of the northern part of the micro continent, using 2D seismic reflection data. Broadband seismic surveys from 2012 and 2011 are used together with older data in order to get an overview of the geological history of the micro continent, with emphasis on the continental margins.

The method of interpretation was initial observation of the seismic lines, then mapping of the important features such as major truncation-surfaces and strong basal reflectors. Finally, the mapped lines were interpreted and linked to geological processes. Five seismic lines that displayed important features were included in the thesis. The general features displayed on these lines were put together and used to create one profile which displays the geological development of the micro continent.

The general development of the micro continent is strongly linked to the continental break ups between Greenland and Eurasia in the Early Eocene and between Jan Mayen and East-Greenland in the Early Miocene.
The result of the Early Eocene breakup was a volcanic margin on the eastern margin of the Jan Mayen area. Accumulation space in the Jan Mayen area was filled in with sediments from Greenland as Greenland and Norway drifted apart, identified in a pre-breaking sequence. Subsequently, the area became subject to significant extension. Sedimentation continued throughout the extensional phase, which was identified in a syn-rifting sedimentary sequence. Eventually, the sea floor spreading to the east of Jan Mayen died out, and a non-volcanic break on the western margin of the Jan Mayen area separated the micro continent from Greenland, and a post rifting sequence was deposited. It is suggested in this thesis that an increase in melt production post-break-up lead to an extensive distribution of volcanic intrusions throughout the Jan Mayen Basin, as well as the area above the eastern continent-ocean transition. The intruded areas are thought to have been areas of weakness in the crust, making propagation for the intrusion easier.

Sammendrag

Jan Mayen mikrokontinentet ligger isolert fra annen kontinental skorpe, sentralt i havet mellom Norge og Grønland. Denne master oppgaven er en seismisk tolkningsstudie av den nordlige delen av mikrokontinentet. Oppgaven bygger på tolkning av nye bredbånd 2D seismiske refleksjons data som har blitt skutt over Jan Mayen området, brukt sammen med eldre 2D survey. Dataene ble brukt til å rekonstruere geologisk historie med hovedvekt på kontinentalmarginene

Metoden som har vært brukt er basert på at man først skal gjøre objektive observasjoner i de seismiske dataene, før man kartlegger viktige detaljer som termineringsflater eller sterke reflektorer over flere linjer dersom det er mulig. Til slutt tar man de kartlagte linjene og tolker dem inn i en geologisk sammenheng. Fem seismiske linjer som viser spesielle og typiske strukturer og trekk i seismikken blir vist i denne oppgaven, sammen med noen eksempler fra andre linjer. Hovedtrekkene fra disse linjene ble brukt til å rekonstruere den geologiske utviklingen til mikrokontinentet Jan Mayen.

Den geologiske utviklingen på Jan Mayen er tett bundet opp til de kontinentale bruddene som har funnet sted mellom først Eurasia og Grønland i tidlig eocene, siden Grønland og Jan Mayen i tidlig miocene.
Bruddet i tidlig eocene etterlot seg en vulkansk margin på den østlige marginen av Jan Mayen. Sedimentasjonsrom ble dannet og fylt igjen med sedimenter fra Grønland mens havbunnsspredningen pågikk, etterfulgt av en fase med omfattende ekstensjon av Jan Mayen området. Sedimentasjonen fortsatte igjennom ekstensjonsperioden og ble identifisert i en syn-rifting sekvens i seismikken. Havbunnsspredningen på østsiden av Jan Mayen døde ut, og startet opp igjen på vestsiden av Jan Mayen etter et ikke-vulkansk brudd mellom Jan Mayen og Grønland. I denne oppgaven blir det foreslått at en økning i smelteproduksjon etter bruddet fører til utstrakt utbredelse av vulkanske intrusjoner i Jan Mayen Bassenget, samt langs kontinental-osean grensen på den østlige marginen. De intruderte områdene er tenkt å utgjøre svakhetssoner i skorpen, noe som gjør det lettere for intrusivene å forplante seg.

Acknowledgement

I would like to thank my advisor Ståle Johansen for excellent guidance and encouragement throughout the work with the thesis. The Norwegian Petroleum Directorate is acknowledged for providing high quality seismic data; a necessity for all the work. Harald Brekke at NPD must be thanked for his role in supporting the work.
My fellow students Øystein Haugen Solbu and Per Inge Bjørkedal Flo who have been working on similar topics, are greatly acknowledged for fruitful geological discussions and welcome distractions throughout the last year.
The other students in Geolabben, in the depths of PTS, are all thanked for help with the geophysical shortcomings of the author, and for keeping the spirits high throughout the last months.
Finally, I would like to thank my family for supporting me in the 17 years of education that I am about to conclude.

Success consists of going from failure to failure without losing enthusiasm.

- ***Winston Churchill***

Contents

Chapter 1 Introduction

Setting

The island of Jan Mayen is located central in the North Atlantic Ocean, to the north of Iceland. It is dominated by Norway's only active volcano Beerenberg in the North and a narrow ridge to the south west. The geology of the island is basaltic, resulting from volcanic activity related to the mid-Atlantic ridge spreading zone.

To the south of Jan Mayen, an N-S-trending ridge called the Jan Mayen Ridge (JMR) is clearly visible on bathymetric data (Figure 1). The ridge acts as barrier between the Norwegian Basin to the east and the Jan Mayen Basin (JMB) and the Iceland Plateau to the west. To the north it is limited by the Jan Mayen fracture zones, and its southern termination is more gradual. While Jan Mayen is considered to have oceanic origins, the JMR and the JMB are believed to consist of continental crust (Kodaira et al., 1998b; Myhre et al., 1984). Due to its size and its separation from other continental crust by oceanic crust they are classified as a micro continent (Péron-Pinvidic and Manatschal, 2010) named the Jan Mayen Micro Continent (JMMC). The evolution of the JMMC is closely related to the extension and rifting of the North Atlantic as it first got separated from the Norwegian margin during the break up in the Early Eocene, and later from the East-Greenland margin during the Early Miocene (Gernigon et al., 2012).

Previous work

The Jan Mayen micro continent has seen several works in the last thirty years, such as the recent Peron-Pinvidic et al. (2012a, b) who uses magnetic and gravimetric data together with reflection seismic, Kodaira et al. (1998b), who used ocean bottom seismic surveys to view the deeper crustal structures of the micro continent, and (Gunnarsson et al., 1989) who provided a general overview of the Jan Mayen geology, development and hydrocarbon potential.
This thesis will provide a fresh view on the micro continent using newly collected data. It was therefore chosen to remain relatively independent of the previous work until late interpretation and discussion in order to maintain an independent view.

Method

The method used in this thesis is based on the basic principle of observation before interpretation. When observing the seismic data initially one should be objective and only consider the seismic itself, without putting it into a larger context. Then, observations that are considered important should be investigated further, and if possible, mapped on multiple seismic lines. Models and ideas based on the observations can be further discussed, and finally compared to other work.
This process is important to avoid model-thinking, where the interpreter has an opinion of

what he should find before viewing the data, and therefore becomes locked to those ideas, missing an important creative element in the work.
As a result of this the layout of this thesis is sorted so that observation of the data comes first, followed by an interpretation section, before everything is put into a broader context in the Discussions chapter. Both observation and interpretation is displayed for a seismic line before moving on to the next line for readability.

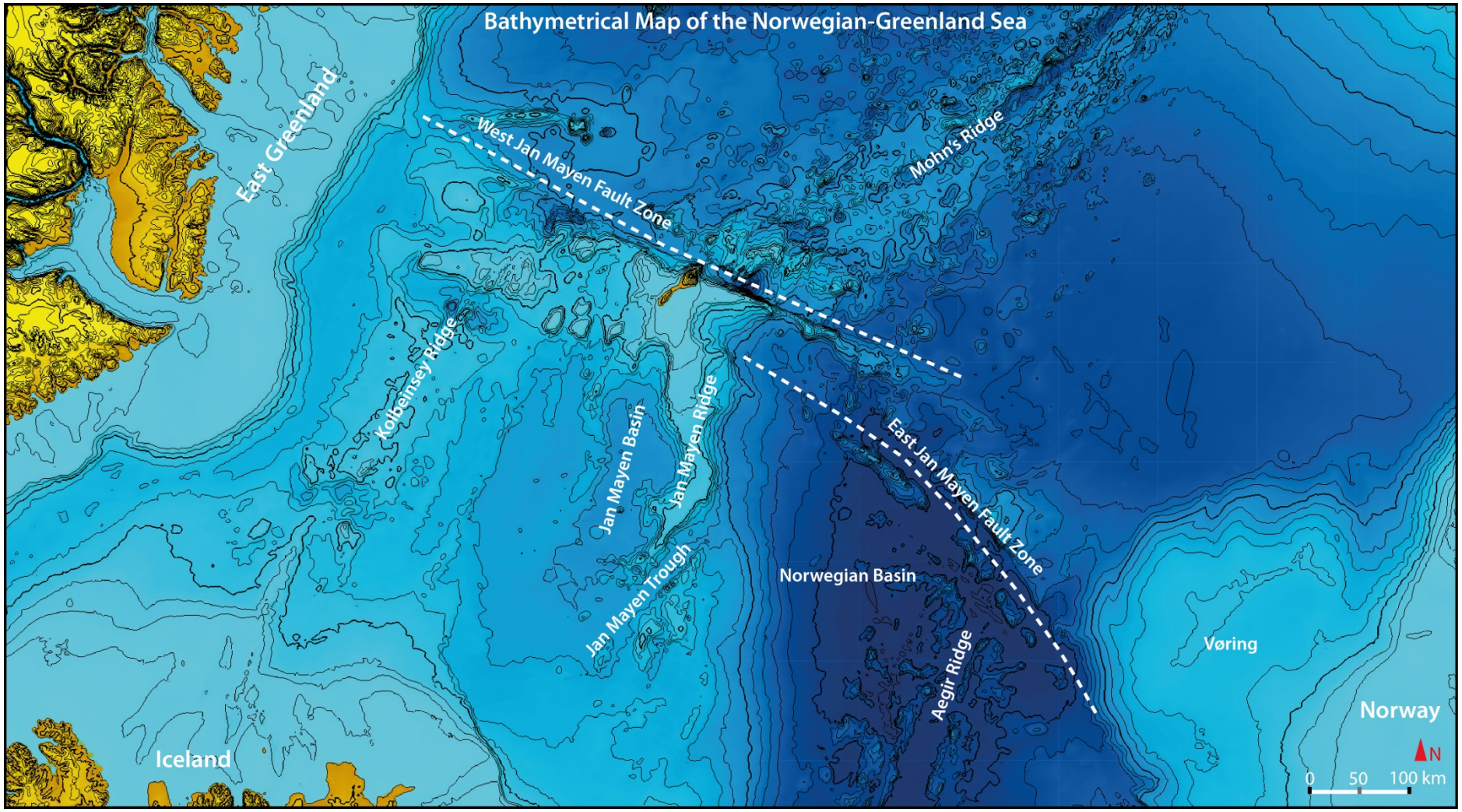

Figure 1. Bathymetrical map overview of the features of the Norwegian-Greenland Sea. Bathymetrical data are from the GEBCO dataset, provided by the Norwegian Petroleum Directorate. Important features in the study area are the Jan Mayen Basin (JMB), the Jan Mayen Ridge (JMR), the Jan Mayen Trough (JMT) and the Norwegian Basin (NB).

Chapter 2 Geologic history of Jan Mayen

Pre-Breaking Tectonics

While Jan Mayen remains a relatively unexplored area the conjugate margins in the Norwegian Sea and the east Greenland has a longer history of exploration. As the areas were connected until the Early Eocene it can be assumed that their geologic history and development before the break up correlates well.

The tectonic history of the Norwegian Sea margin can be dated back to the Devonian, with the collapse of the Caledonian mountain chain and several periods of extension and rifting later.

The structural elements that are visible today on the Norwegian Margin were first activated in Permian to Carboniferous times (Brekke, 2000). In the mid-Permian significant extension and normal faulting have been recorded in East Greenland, while the Norwegian margin has extensive faulting in the late-Permian and early Triassic (Faleide et al., 2008). In the Late Triassic and Early Jurassic there was general tectonic quiescence with deposition in basinal areas. Previous work has estimated the province of basins in the pre-Late Jurassic to be less than 400 km wide. (Skogseid et al., 2000) In the late Jurassic and early Cretaceous the African and American plates had begun to break apart in southern and central parts of the Atlantic, and the motion continued as rifting and extension in the North Atlantic. It has been estimated that the continental crust was stretched by approximately 60 km in this period of rifting (Skogseid et al., 2000). The extension lead to the creation of extensive Cretaceous age basins on both east Greenland and Norwegian margins which constitutes the main NE-SW structural trend seen on the margins today (Faleide et al., 2008).

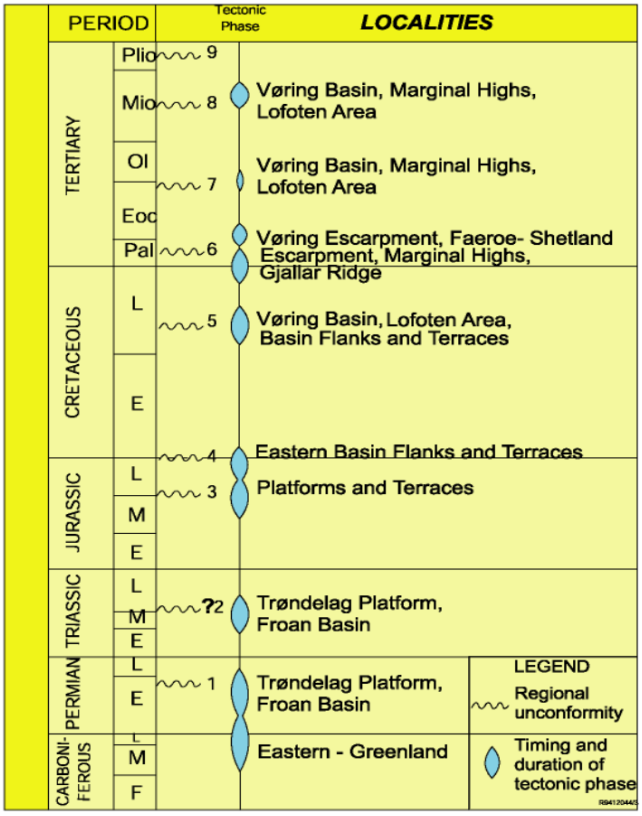

Figure 2. Tectonic development of the Norwegian margin. From (Brekke, 2000).

Breaking of the North Atlantic

As a result of the repeated extension and rifting sequences in the North Atlantic, the continental crust was stretched thin, and a final stage of rifting throughout the late Cretaceous, Paleocene and Early Eocene was therefore able to separate the continental plate into two separate parts, Greenland and the Eurasian plate. The breaking is estimated to have occurred in the Early Eocene at about 54-55 Ma. (Gernigon et al., 2012) (Faleide et al., 2008) (Brekke, 2000) (Mjelde et al., 2008a). It leads to 3-6 Myrs of intense volcanism along the Norwegian margin, and the initiation of oceanic crust generation. The oceanic crust was initially generated at the Aegir ridge off the mid-Norwegian margin, and the Mohn's Ridge further north. The two ridges are separated by the East and West Jan Mayen fracture zones (Figure 1). The East JMFZ represents the spreading trend of period of approximately 30 Ma from c. 55 Ma when the Aegir ridge was an active spreading center together with the Mohn's Ridge. (Kuvaas, 1997; Mjelde et al., 2008a) This period ended when the spreading at the Aegir Ridge ceased and the Kolbeinsey Ridge activated along the eastern margin of Greenland in the Oligocene around 25 Ma (Gernigon et al., 2012). Based on recent aeromagnetic data from the Norwegian Basin, Gernigon et al. (2012) divided the development of the Aegir Ridge into two phases (Figure 4). Phase one is the initiation of seafloor spreading and associated magmatism from 53.3 Ma-49.7 Ma. Phase two describes a change in growth direction as well as a slower spread rate of the oceanic crust. The changes resulted in that the oceanic crust grew in a fan-like shape widening towards the northern parts of the basin. To compensate for the differential growth, the southern part of the JMMC was subject to extension, giving rise to the ridges seen on bathymetric maps of the JMMC today. This means that throughout the Eocene and Oligocene, East Greenland underwent extension and rifting at the same time as sea floor spreading was occurring along the Aegir Ridge, resulting in a thinning of East Greenland's continental crust (Kuvaas, 1997). Kuvaas (1997) suggested that the extensional period ended with a regional uplift and erosion just before the onset of seafloor spreading along the Kolbeinsey Ridge at c. 24.5 Ma. With the generation of oceanic crust at the Kolbeinsey Ridge, separating the Jan Mayen area from the East Greenland margin, it became an actual micro continent as it is classified today.
Due to its tectonic history it is reasonable to assume that the Paleozoic and Mesozoic geology of the JMMC is shared with both the Norwegian Margin and East Greenland until the Early Eocene, and that it's Eocene and Oligocene history is shared with Eastern Greenland.

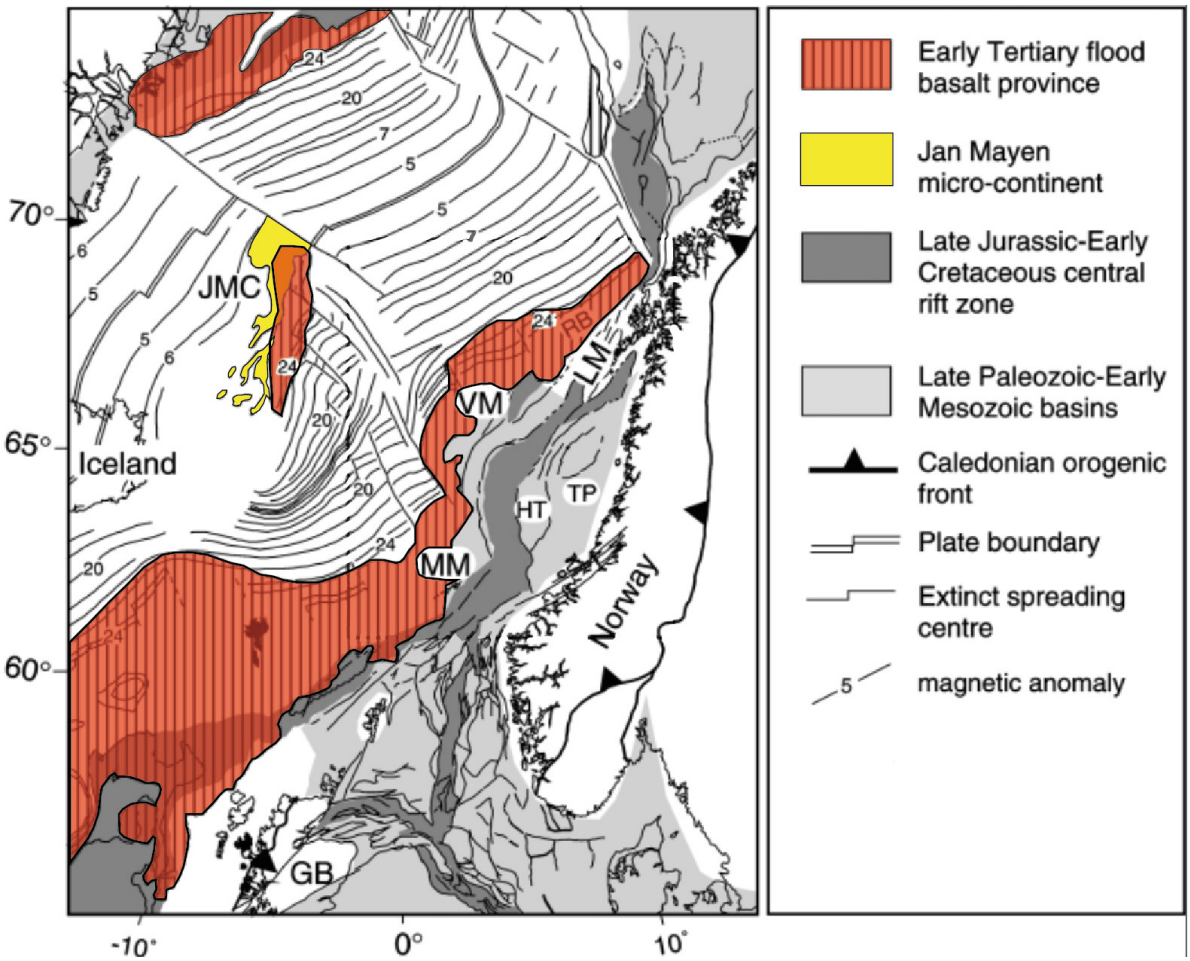

Figure 3. Extent of the Early Eocene basalt floods and today's location of the JMMC. Notice how the conjugate margins on East Greenland, East Jan Mayen and the Norwegian Margin correspond to each other, and the lack of volcanism on the western side of JMC. Modified from C. Berndt (2001).

Volcanism during the breaks

Most of the work that has been done on the factors controlling the sea-floor spreading in the North Atlantic concludes that a mantle plume called the Iceland mantle plume is central in the development of the spreading ridges. A mantle plume is a part of the mantle with increased thermal gradient. Due to partial melting an increase in mantle temperature of about 50 degrees C will cause an increase in the amount of melt produced of around 50 % (Parkin and White, 2008). A larger amount of melt produced leads to more volcanism and a thicker oceanic crust when sea-floor spreading is initiated.

The Aegir Ridge saw a significant production of both magmatic material and oceanic crust, and is considered a volcanic passive margin (Myhre et al., 1984). According to Breivik et al. (2006) a burst of significant initial magmatic activity lasted for about 2.5 Myr. This was reflected by the half rates of sea-floor spreading in the Norwegian Basin; It changed from an initial 30 mm/yr in between magnetic anomalies C23 and C24B, 15-19 mm/yr until C20, and a slow 6-8 mm/yr production which lasted until the Aegir Ridge became extinct. Breivik et al. (2006) attempt to explain the decrease in magmatic activity over time by including a measurement of a NE directed flow in the asthenosphere along the ridge. Further south, along the Greenland-Iceland-Faroe Ridge, the mantle had been depleted by excessive volcanism, and when the asthenopheric flow brought this depleted mantle to the Aegir Ridge, the production of melt died down.
Mjelde et al. (2008b) stated that during the period of significant volcanism just after the initialization of sea-floor spreading at the Aegir ridge, the oceanic crust that was produced has been reported to be unusually thick and that this was related to an increase in the temperature of the underlying mantle. Saunders et al. 1997 and Jolley and Bell 2002 estimated initiation of the mantle plume activity ca. 5 Myr before Early Eocene continental breakup, as summarized by Parkin and White (2008). This fits well with Gernigon et al. (2012) who stated that the volcanism happened in two phases; the first from 63 to 55 Ma was characterized by magma with contamination of continental crust, and the second from 55.3 to 53 Ma with much less contamination, suggesting that the generation of oceanic crust had started (Saunders et al., 1997). During the second stage of volcanism, seaward dipping reflectors (SDR) were generated by the massive amounts of vulcanite together with sills and dikes intruding into older rocks (Faleide et al., 2008). Such SDR sequences have also been reported to exist on the eastern margin of the JMR. (Kuvaas, 1997; Peron-Pinvidic et al., 2012a). In the earliest SDR sequences there are traces of continental contaminations, but this generally lessens in the younger basalt floods, reflecting the transition to ocean floor spreading (Eldholm et al., 1989; Saunders et al., 1997).

The Kolbeinsey Ridge is considered a non-volcanic passive margin (Kodaira et al., 1998a; Kodaira et al., 1998b; Mjelde et al., 2007; Mjelde et al., 2008b), and the initial spreading of the ridge generated thin oceanic crust for the first 2 Myr. However, after ca. 23 Ma the produced crust increased in thickness to ca. 8 km, above the global average of 6 km (Mjelde

et al., 2008b) and it is still producing at the present time. Based on a relationship with spreading rates and crustal thickness Kodaira et al. (1998a) estimate the temperature of the mantle source of the Kolbeinsey ridge to be 20-60 degrees C warmer than average mantle. Kodaira et al. (1998b) found that the thick crust generated by the Kolbeinsey Ridge after its initial slow start was caused by an increase in the melt generation as a result of the increased temperature in the mantle related to the Icelandic mantle plume. The lack of volcanic activity initially is explained to be a result of a long rifting period before the break, where the heat was conducted away and little additional melt was generated. Another factor that could account for the changes in volcanic activity along the Kolbeinsey ridge, and the Aegir Ridge, is pulses of temperature variations in the mantle plume (Mjelde et al., 2008a; Parkin and White, 2008), which would lead to variations in the thickness of the crust. Mjelde et al. (2008b) suggests that the initial seafloor spreading along the Kolbeinsey Ridge happened during a time of low temperature that lasted from the late Eocene to Oligocene. Then, the mantle plume activated again and the increased temperature resulted in more melt, and thicker oceanic crust. In the paper it is also stated an alternate explanation, where the change in melt production is caused by that the mantle plume did not fully interact with the Kolbeinsey Ridge until 23 Ma.

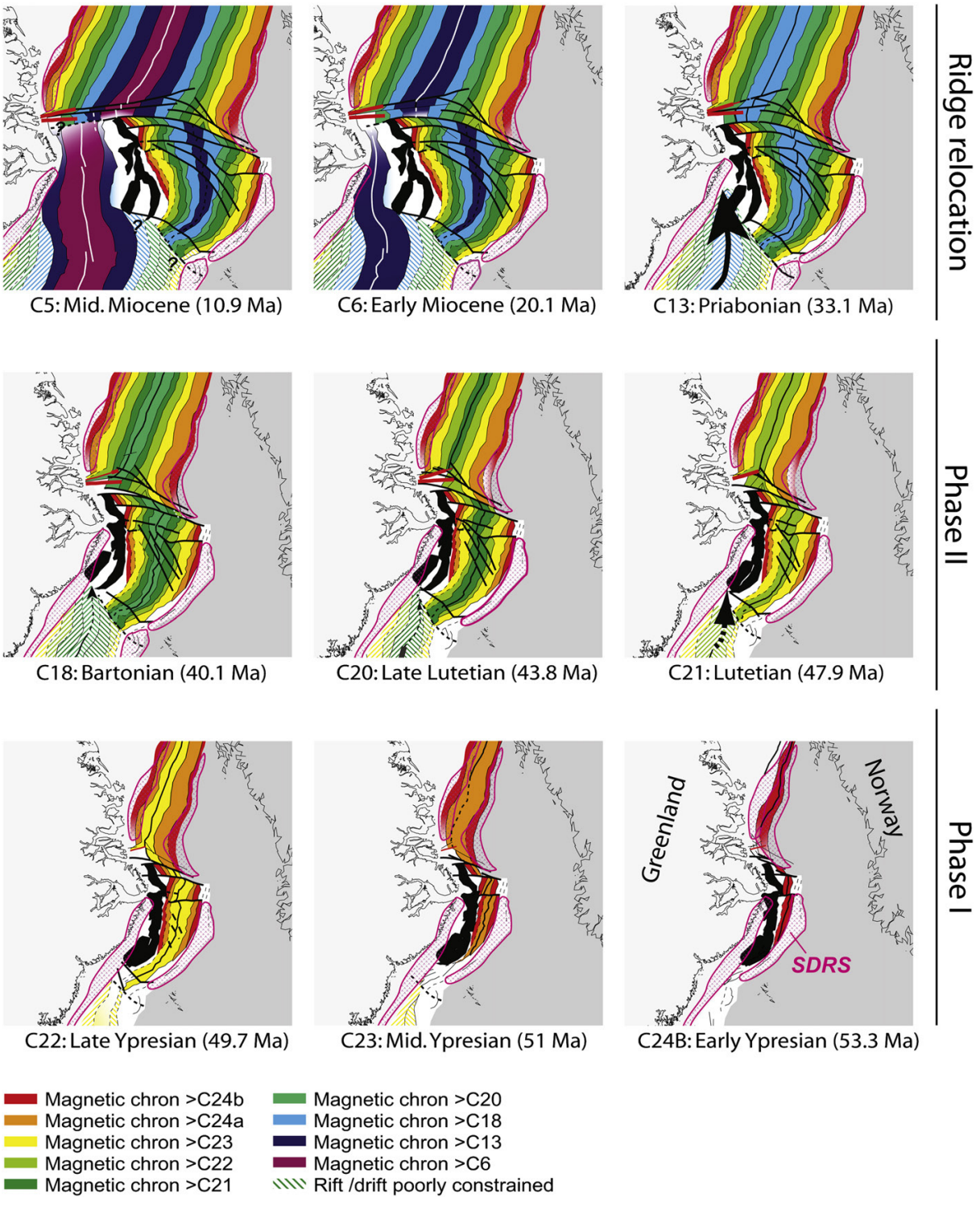

Figure 4. Development of mid ocean ridges in the North Atlantic. Notice the rapid spreading in Phase 1, the fan-like spreading shape in phase two and the relocation from the Aegir Ridge to the Kolbeinsey Ridge. From (Gernigon et al., 2012).

Chapter 3 Relevant geological processes

Volcanic facies at a volcanic rift zone

Planke et al. (2000) summarized a series of papers to develop a term called seismic volcanostratigraphy, and gave a description of the most significant extrusive volcanic facies found at volcanic rifted margins. They conclude that the main factor in determining which volcanic facies will be deposited from extruded magma is the presence of water. Five stages of volcanism with distinctly different facies were described (Figure 5);

The first stage describes the initial volcanism and the results of contact between magma and wet sediments in a rifted basin. The result is an explosive type of volcanism with deposits that are a mixture of sediments and vulcanite.

The second stage consists of subaerial flows of lava that respond to its surroundings. The topography is filled in with sheets of basalt floods, and lava deltas may form along the coast where the floods come into contact with the water.

The third stage results in the development of the inner SDRs. The SDR sequences are believed to be deposited lava flows formed by either the Mutter or the Hinz models (Figure 6) (Mutter, 1985; Planke et al., 2000).

By Mutters model, the SDR sequences are formed as a subaerial seafloor spreading zone, meaning that they are a part of the ocean crust, and that the continent-ocean boundary (COB) is located on landward end of the SDR sequence. The dip towards the spreading axis is caused by loading of new flows weighing down the previous flows. When the spreading axis is submerged below sea level, the length of the flows is reduced and deposition of the SDRs ceases.

Hinz suggested that the SDRs were formed as a result of fissues of subaerial volcanism with lava flowing over continental crust. As in Mutters model, the dip is ensured by subsidence as a result of loading by the deposited lava flows. The SDRs ceases to be deposited when the volcanic fissue begins producing ocean crust, and as such the COB would be located at the seaward end of the SDR sequence.

While Mutters theory has successfully been applied at Iceland, it has been determined by seismic and well-data that the SDR-sequences may be underlain by continental crust on the Vøring margin (Eldholm et al., 1989), and observation of SDRs perpendicular to the JMFZ on the Vøring margin confirm that they may be deposited outside of a spreading zone (Planke et al., 2000). It is therefore believed that the process leading to the SDRs deposition is an interaction between the volcanism and its creation of new continental crust together with the tectonic processes linked to the extension of the continental crust (Planke et al., 2000). As the deposition of the basalt sheets in the sequence follow the topography at the time of deposition, local variations in the extent of the SDRs can be large. Planke et al. (2000) also describes strong reflections close to perpendicular to the dip of the SDRs at the seaward base of the SDR sequences which they interpret to be dikes propagation along faults. Towards the seaward end, the SDRs often appear to terminate in an area of chaotic reflections called the Outer High by Planke et al. (2000).

The fourth stage represents the deposition of the Outer Highs. Well data interpreted by Shipboard Party, 1984, and summarized by Planke et al. (2000) suggest that the Outer High was deposited in a shallow marine environment, and that it consists of both volcanic material and reworked volcanic sediments. As the spreading center sank below sea level due to subsidence the volatility of the eruptions increased, resulting in a fragmented and inhomogeneous structure which turns out as chaotic on seismic.
The fifth stage takes place when the spreading axis is submerged into a deep marine environment. The explosive nature of the eruptions seen in the shallow marine settings is no longer possible due to the hydrostatic pressure, and the volcanites are therefore believed to form basaltic sheet flows, similar to the ones seen in the Inner SDR, and they are thus called the Outer SDR sequence. The Outer SDR can be distinguished from the Inner by a smoother top basement that connects directly to the ocean crust basement and by its location on the seaward side on an Outer High (Planke et al., 2000).

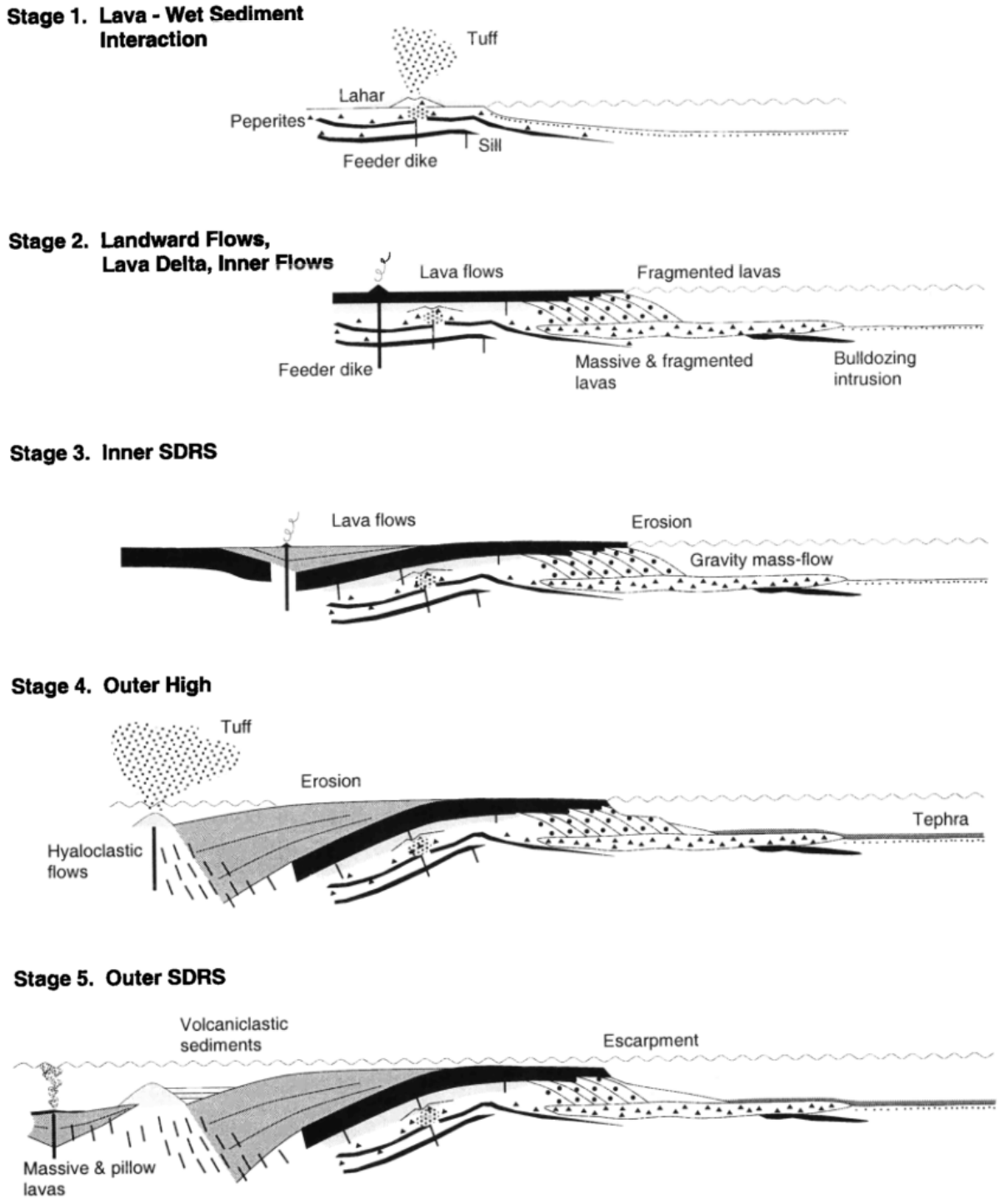

Figure 5. Model of the timing and placement of volcanic facies, related to volcanic rift margins (Planke et al., 2000).

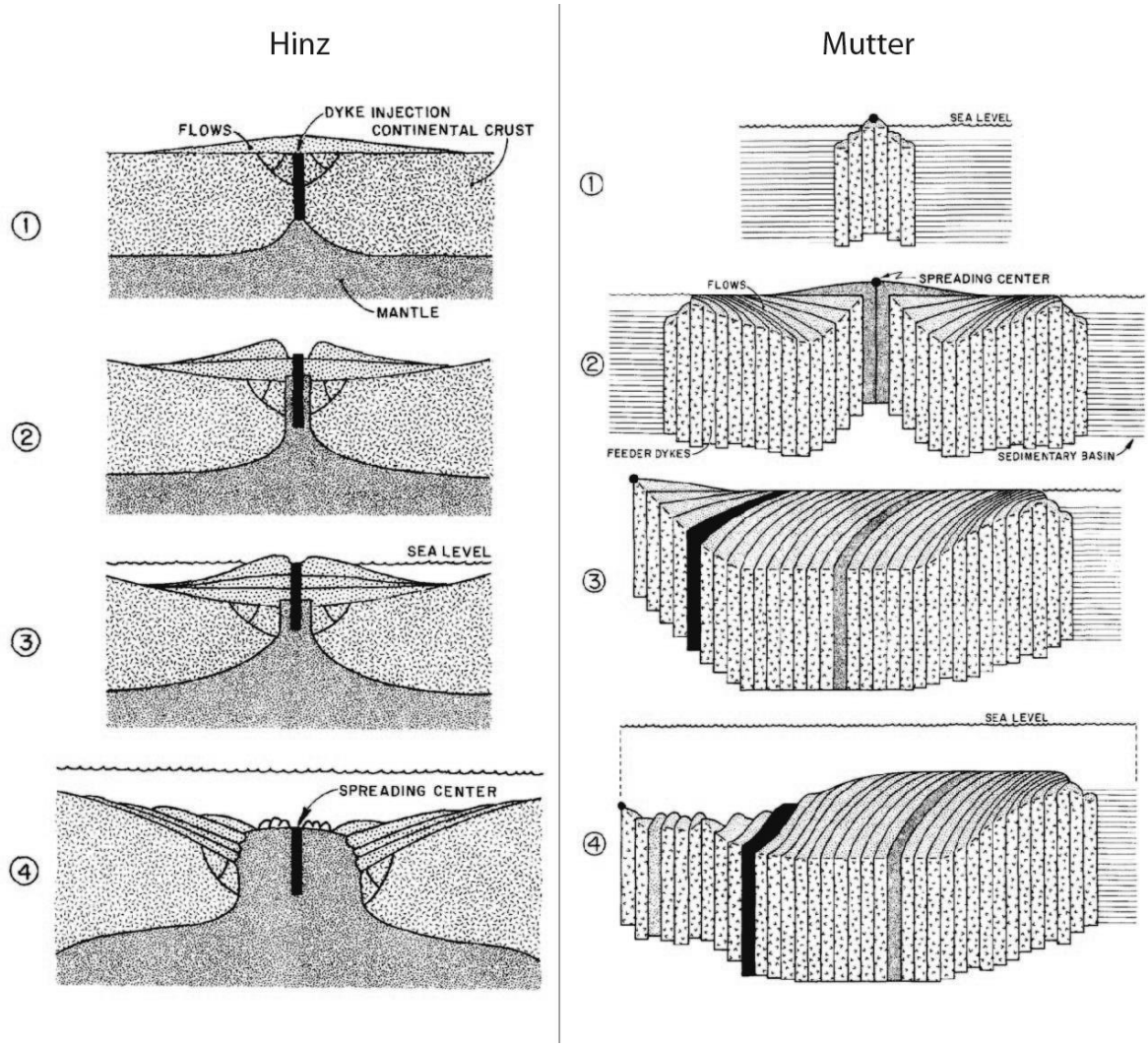

Figure 6. The models for SDR-generation presented by Mutter and Hinz. Note that the two models predicts different locations of the COB; according to Mutters is lies at the landward end of the SDR-sequence, while Hinz predicts it is further out near the seaward end of the SDRs. Modified from (Mutter, 1985).

Intrusions

Magmatic intrusions are deposits of magma that has intruded and eventually solidified along cracks within a host rock. They are commonly divided into dikes and sills. Dikes are intrusions along cracks cross-crosscutting the stratigraphy, while sills are intrusions following the stratigraphy of the host rock. Intrusions may propagate along already existing fractures in the rock, or induce their own pathways (Rubin, 1995). In order for an intrusion to form in a previously created fracture the pressure of the magma must be larger than the compressional forces perpendicular to the fracture. In order to induce fractures in the host rock the magmatic pressure needs to be larger than the minimum compressive stress, and will then form intrusion perpendicular to the direction of the minimum stress. If the magmatic pressure rises above the pressure of the largest compressional stress the fractures may open in any direction (Rubin, 1995) Magmatic intrusions are a common feature of volcanic passive margins, including the North East Atlantic.

Saucer shaped intrusions is an intrusion-geometry which has been described at the Norwegian margin (Polteau et al., 2008b). The saucer shape contains three main segments; the inner sill forms the main body of the intrusion, the inclined sheet cuts up through the host rock along the outer edges of the inner sill, and the outer sill protrudes from the top of the inclined sheet As Polteau et al. (2008b) summarized Chevallier and Woodford, 1999). Often, doming of the layers of rock above the saucer-shape is visible. Polteau et al. (2008a) found that the intrusion is likely fed by a feeder in the center of the shape. Several models exists on how the saucer-shape is obtained. Experimental modeling done by (Galland et al., 2009) suggest that the geometry is caused by a process where the inner fill expands, causing doming of the overlying layers. The differential uplift at the inner sill edges causes shearing forces which eventually causes faulting. The propagation of the intrusives in the inner sill is directed up the faults and the inclined sheets are formed. The experiment also proposed that the saucer-shape is dependent on depth, and that the extent of the inner sills tend to increase with depth, a trend which is also observed in outcrops (Polteau et al., 2008b). Malthe-Sørenssens et al. 2004, summarized by Polteau et al. (2008b), found that there is an relationship where the inner sill is 4-5 times the thickness of the overburden at the time of the emplacement.

Figure 7. Schematic of a saucer-shaped intrusion (Polteau et al., 2008b).

Chapter 4 Data and data quality

The data used for this master thesis consists almost exclusively from reflection seismic. Access to well data is limited as no deep wells have been drilled on Jan Mayen. Three wells drilled by the deep sea drilling project, sites 347, 346 and 349. The well report for site 349 was used to determine the age of an unconformity in the seismic data.

5 2D reflection seismic surveys from Jan Mayen have been used for this project and one from the Møre margin, all kindly supplied from the Norwegian Oil Directory. The lines provided a good overview of the Norwegian part of the JMMC, especially around the JMR (Figure 10). Most of the lines have been shot perpendicular to the north-south trending JMR, and a few shot in a north-south direction. Three of the surveys are new data, 2 shot in 2012 and one in 2011, both shot by PGS. Compared to the other available surveys from 1988 and 1979 the resolution and quality of the seismic is much better as seen in the comparison in Figure 8 where the two lines are separated by only about 800 m. The most recent data have therefore been used as the main input for the project, while the other surveys used were as support in interpretation.

The 2011 data is overall of very good quality. The 2012 surveys on the other hand suffers from what is probably a bad velocity model used in the migration of the data producing migrational “smiles” (Zhu et al., 1998). The issue mainly affects the lower reflections in the datasets, adding uncertainty to any interpretations in those areas. An example of the problems may be seen in Figure 9.

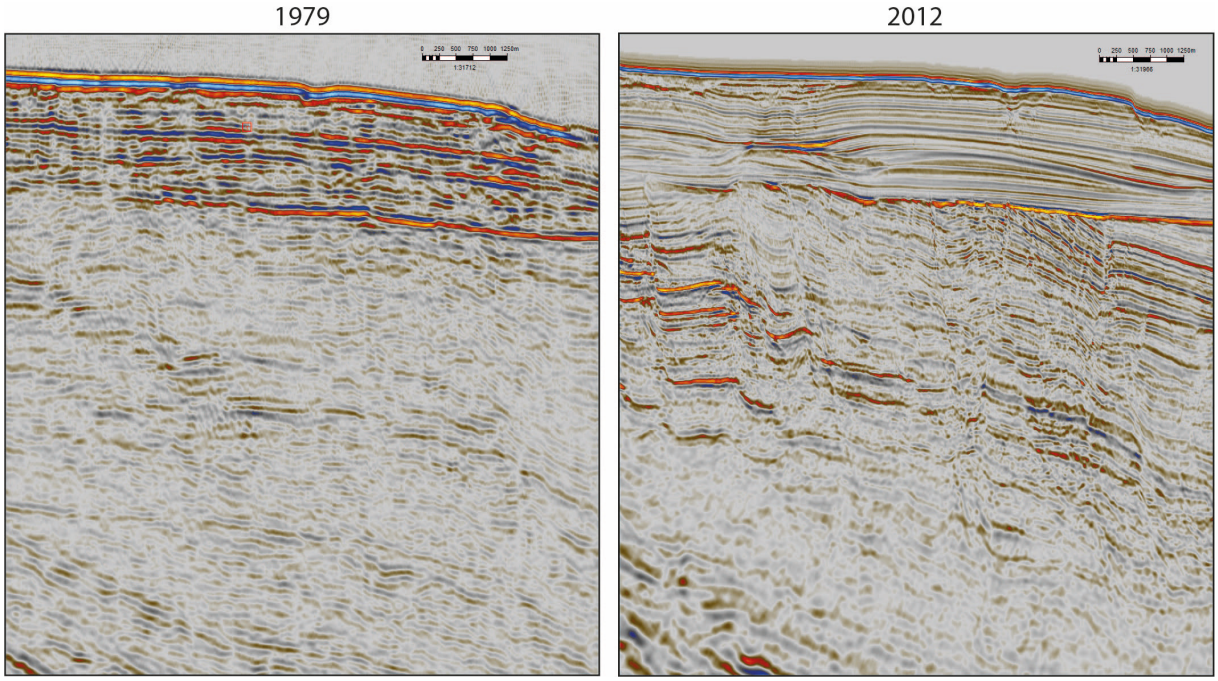

Figure 8. Comparison between 1979 seismic and 2012 broadband seismic from the Jan Mayen Ridge. The Lines are about 800 m apart.

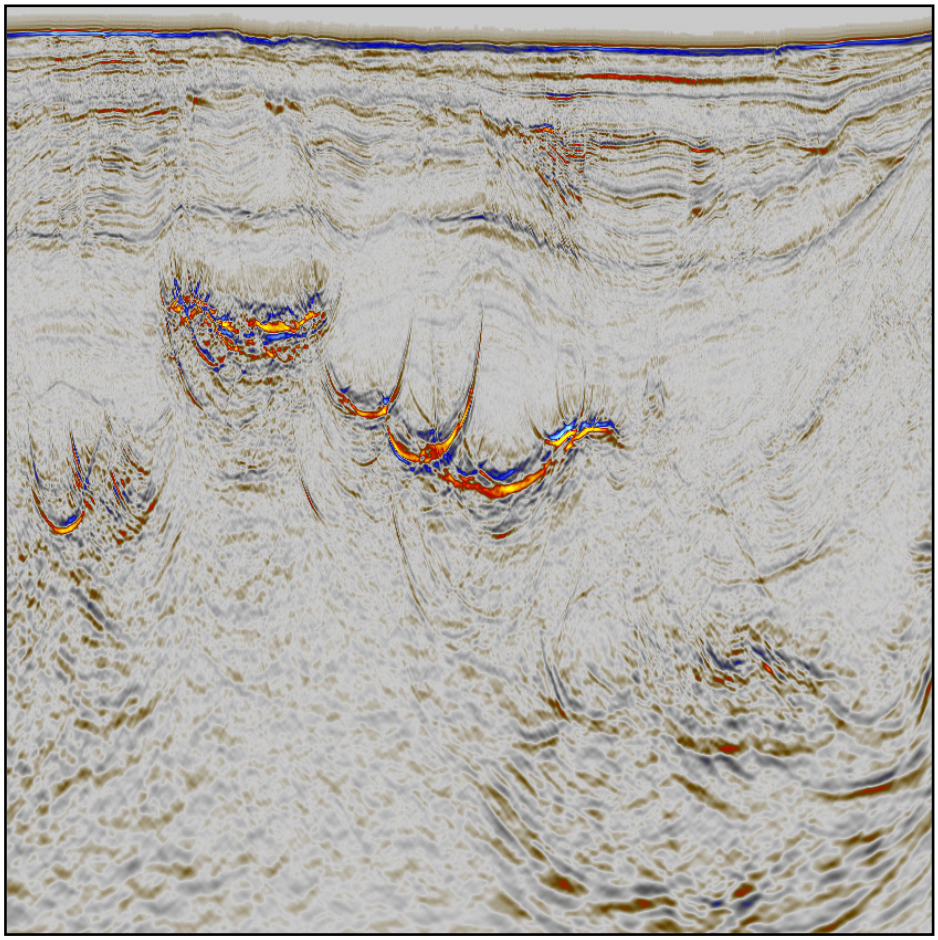

Figure 9. An example of migrational smiles in the 2012 data. The bright reflector is likely a volcanic intrusion in a sedimentary basin. Also notice the low quality of the reflections from the lower right.

Challenges of basalt imaging

Intra and sub-basalt seismic imaging is problematic due to the rock properties and lithology of the basalt deposits. One of the main issues is that the seismic velocities in the rock have great variations, the same melt can produce rocks with p-wave velocities varying from 1.5-7.5 km/s (Planke et al., 1999). This variation is largely dependent on the type of emplacement process: Intrusions are generally homogenous with velocities of 5.5-6.5 km/s. And both velocity increase and decrease may be seen in the surrounding host rock as a result of alteration and fractures. Sub-aerial flood basalts are more diverse, and display a great velocity increase from the exterior of the flow (2-3 km/s) to the interior (5-6 km/s). The thicker the flow is, the higher the average velocity of the volcanic unit. Velocity differences are also seen between flows of similar thickness. The variation was interpreted by Planke et al. (1999) to be a result of heterogeneity and anisotropy of the basalt rocks.

The strong impedance contrasts between sedimentary rocks and volcanic rocks leads to that a lot of the seismic energy is reflected, both when going down and up, causing little data from below volcanic deposits. The heterogeneity seen in flood basalts would also degrade the seismic.

Overview of the data

The available data, together with the sections displayed in the thesis are highlighted in Figure 10.

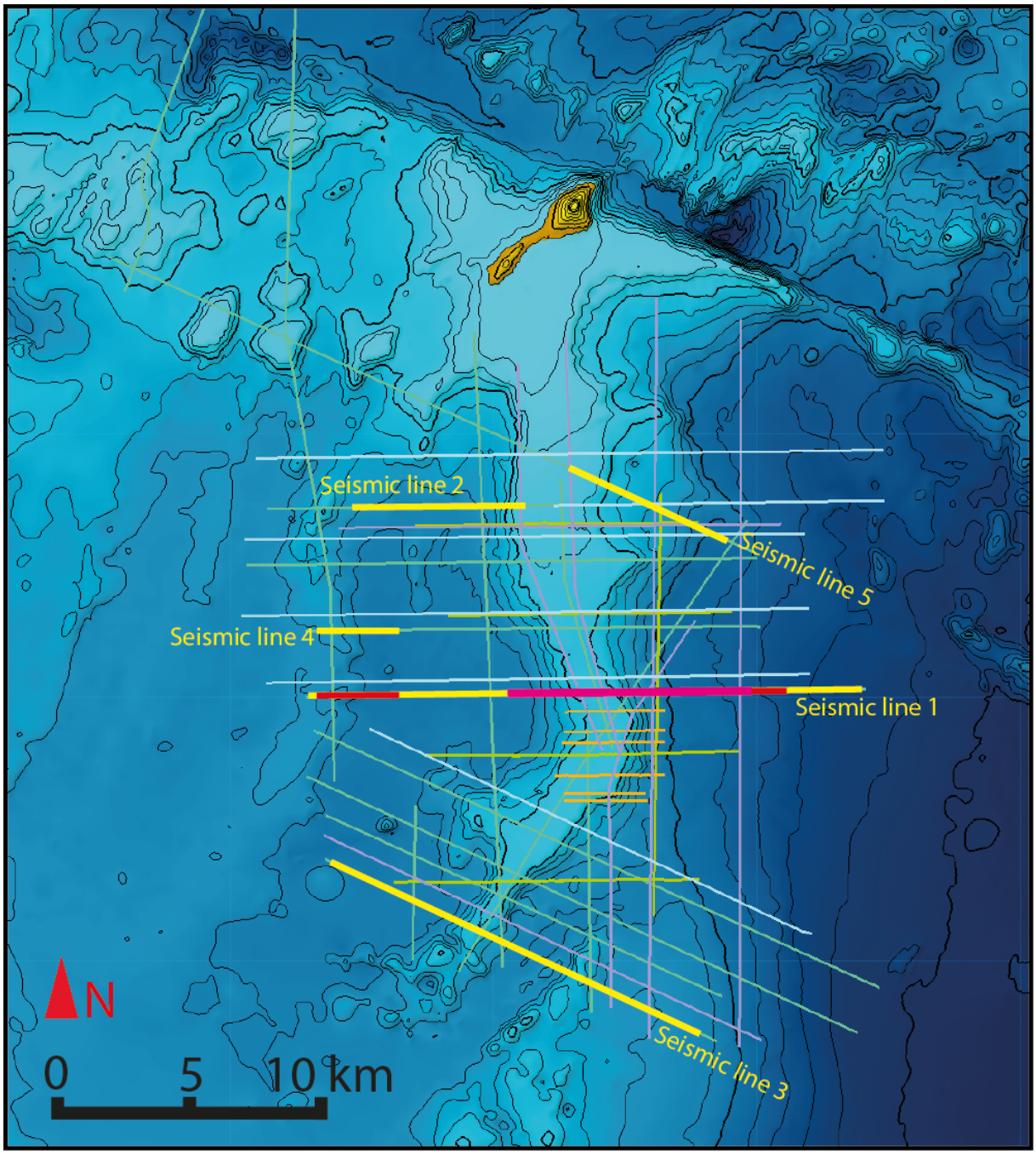

Figure 10. The dataset available. Thick yellow lines are the sections displayed in the thesis. The red lines are the sections displayed from seismic line 1.

Chapter 5 Observation and interpretation of seismic data

Seismic line 1

Seismic line 1 displays a line crossing the JMR east to west at 69˚29. Initial observations suggests that the seismic section may be divided into three regions laterally; west of the JMR, east of the JMR and the JMR including its transitional zones towards the other regions. Three seismic sections representing the regions are included in the thesis.

The western section of seismic line 1

The westernmost parts (Figure 11) are recognized by a horizontal sea bottom reflector that stays at a depth of approximately 3 s. There are few features in the underlying seismic except for one prominent reflector at 3.5 s (Reflector 1, R1). The reflector is a hard event with high amplitudes compared to the rest of the survey. The top of the reflector is relatively clearly imaged, unlike its lower parts which appear chaotic giving it a thick appearance. It consists of a series of near horizontal sections with lengths of up to 10 km that are shifted vertically up to 0.2 s if compared to each other. The eastern and western ends of R1 are at approximately the same depth. The seismic is highly chaotic below R1, and no consistent reflectors can be identified. In some areas hard events which tend to bend upwards laterally can be seen, but not followed over long distances. The reflector terminates when reaching the lower flank of JMR in the east, and towards another high in the west.

The high in the west (Figure 11) is characterized by a strong, hard reflection which divides it into an upper and a lower part. The upper part consists of sediments similar to those seen above R1 to the east and the lower part is highly chaotic with no reliable reflections. Reflections to either side of the high terminate when approaching the steep discontinuities that constitute the slopes of the high.

The interval between R1 and the sea bottom has two main parts where the lower is highly chaotic and relatively low amplitude, and the upper half consists of several medium amplitude consistent reflectors. The reflectors are frequently shifted vertically along vertical or near vertical lines, and the shifts affect the sea bottom to some degree. Some of the more significant vertical shifts appear at the same places as the vertical shifts in R1, but the displacement seems smaller. The interval thickens by ~ 0.25 s when approaching the transitional area towards the JMR.

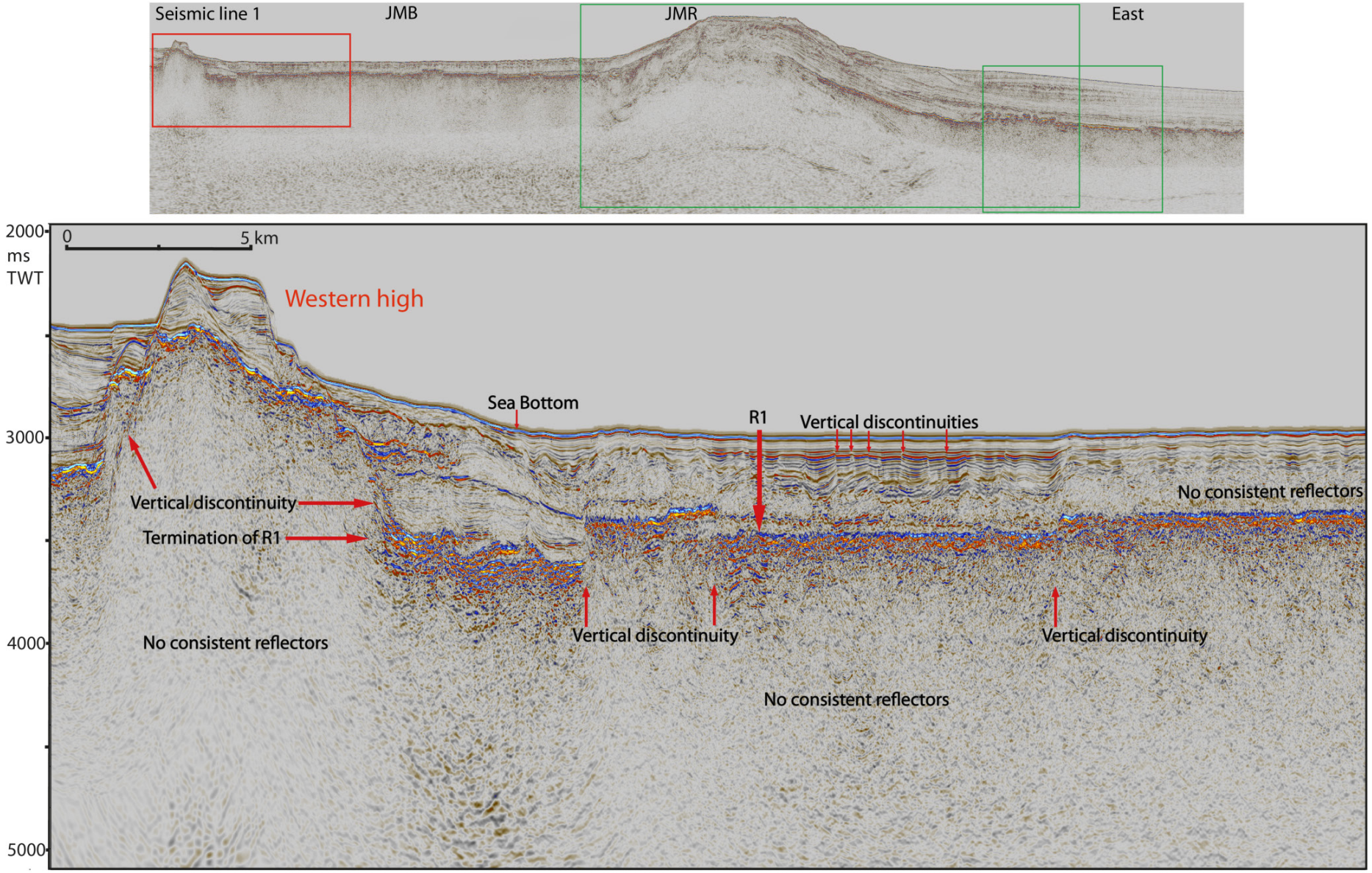

Figure 11. The westernmost section in seismic line 1, as marked by red in the upper marked image Note the transition from the R1 reflection to the thinner and cleaner reflector on the high. Also note that the group of reflectors to the east of the high that terminate against the vertical discontinuity that constitutes the eastern flank of the high.

The eastern section

The sea floor in the eastern region is dipping slightly away from JMR. It can be divided into three main parts vertically, see Figure 12.

The bottom interval is a zone of low amplitude chaotic reflectors. Most of the reflectors are inconsistent, except for one (R2) which stands out clearly at a depth of about 8.2 s TWT, or about 4.6 s TWT from the sea floor. It is not continuous through the entire section, but terminates abruptly in both easterly and westerly directions. R2 is dipping slightly upwards in both directions from a middle point, and it should be noted that the dip is inconsistent with other reflectors in the section.

The middle interval of the eastern section has an upper boundary marked by a high amplitude reflector (R3) at a depth varying between 5-6 s. In the western part of the section, the reflector is highly irregular, displaying jumps up and down with depth-variations of about 0,25 s. The jumps happens ca. every 1 km, and the elevated parts of the reflector are also about this length. The elevated parts pinch out to the sides, and do to some degree display an upwards dip at their ends. The whole section of these irregular reflectors is about 12,5 km long. From the eastern termination of the irregular reflectors, R3 changes appearance to a more coherent high amplitude reflector visible in the middle of the section. Moving eastwards the reflector does some vertical shifts of about 0.1 s, and gradually becomes weaker and more inconsistent, before it is shifted down to about 6 s in the far eastern parts of the section. Below the reflector the seismic is chaotic, and no consistent reflections may be identified.

The third interval in the east region is limited by R3 downwards and the sea floor upwards. Fairly consistent reflectors may be observed in the entire interval, but with some varying characteristics, used to divide it into several sub-intervals.

The lower part, subinterval 3.1, from R3 and ~0,3-0,1 s up, displays fairly high amplitudes and coherent reflectors that dip eastwards . In the section just above the irregular part of R3, the reflectors seem to bend around or get uplifted by the shape of the uplifted parts of R3. The anticline-like structures continues to affect the reflectors above until it appears to be terminated when reaching the top of sub-interval 2 The effect weakens upwards. It is also possible to see some reflections in between the uplifted sections of R3.

Sub-interval 2 is characterized by relatively low amplitudes with reflectors dipping slightly gentler than the underlying sub-interval. The dip is gentling farther away from JMR.

The third sub-interval is marked by fairly high amplitudes west in the section, which changes and turns lower towards the east. The reflectors are somewhat chaotic due to an extensive amount of near vertical displacement lines, disturbing the continuity of the reflectors. One hard event at about 4 s seems to be relatively unaffected by all the disturbances and continues through the section from west to east, but turning weaker towards east (R4). The seismic closest to the sea floor appears smoother than what is seen further down.

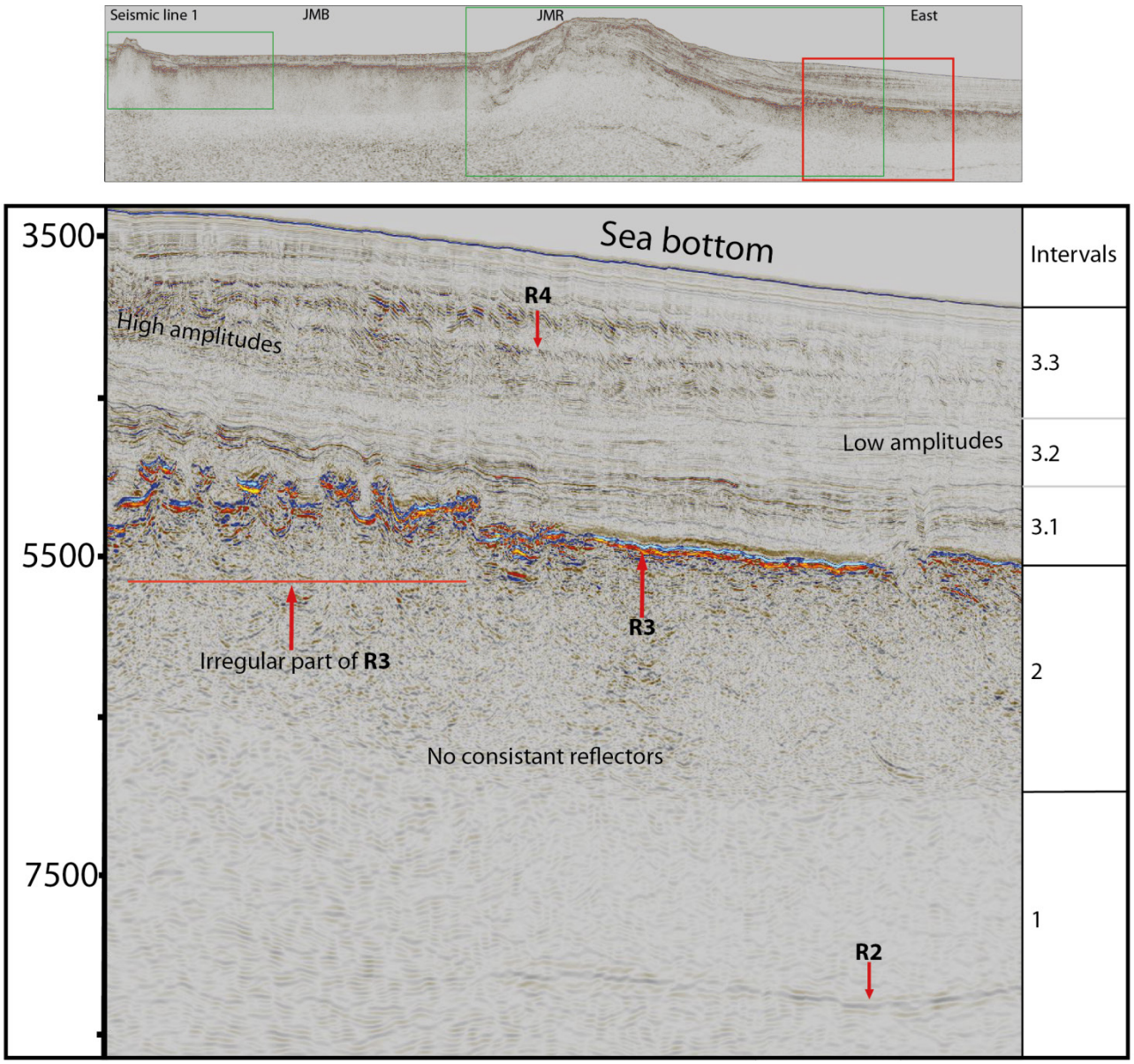

Figure 12. The eastern seismic section from seismic line 1. Note the opaque R3 reflector and its irregular part. R2s location in an otherwise data-free area should also be noted.

The middle section of seismic line 1

The middle region is more complex than the other two, with the JMR in the middle, and slopes down towards the JMB in the west and the NB in the east. In general reflections from the eastern slope are more continuous and better imaged than the reflectors on the western slope. They also appear to dip downwards towards the NB at a gentler rate than at the JMR-JMB-slope.

The section may be divided into the same three intervals as used in the eastern section. The two lower intervals are separated from the upper by a set of high amplitude reflectors that are the continuation of the R3 reflector seen in the eastern section (Figure 12). On the eastern slope, R3 stands out as a strong and clear reflector, but from the top of the slope and westwards it becomes less pronounced and hard to follow.

The lower interval 1 consists mostly of chaotic, low amplitude, low frequency reflectors. Somewhat similar to reflection R2 (Figure 12), a reflection stands out in an area where the surrounding seismic is characterized by low amplitudes and chaotic reflectors. Three different segments at similar depths, about 6.3 to 7 s, with similar appearances may be observed, and they have all been marked as R5 in Figure 13. The eastern segment of R5 seems to be dipping towards east, the western towards west, and the middle one appears horizontal, all following the trend of the ridge above.

To the east of the eastern R5 segment, a reflection set (RS2) which dips down towards the ridge is visible, contrary to the other reflections in the area. The reflections are smooth and low frequency, but with varying dip-angles.

As they get closer to R3, the amplitude of the chaotic seismic tends to increase. Some data may be identified below the high amplitude parts of R3, including a set of reflectors (RS1) that display a dip towards the east that is far steeper than R3 and the overlying reflectors. While the reflectors may not be traced all the way up to the overlying R3 reflector, some weak reflectors and the general dip of the smaller chaotic reflectors closer to R3 indicates that the dip continues all the way up. Further west the dip appears gentler, but still steeper than the overlying R3.

Below R3, more reflections may be seen all the way from the western slope and over the ridge to the east. They are generally low amplitude (Figure 13), and it is difficult to trace any reflections over a large distance. They seem to terminate in the east when reaching in between RS1 and another strong reflection, R7, which has a gentler dip towards the west.

In interval 3 above R3, the seismic is characterized by consistent reflectors. Based on amplitude variations, seismic signature and truncation surfaces it is possible to utilize the same sub-intervals used in the eastern section.

Sub-interval 3.1 is identified by a package of similarly dipping, medium to high amplitude reflectors that may be followed all the way from the eastern part of the survey and up on the JMR where it is disturbed by several significant vertical discontinuities. At the top of the interval, reflections can be seen terminating into a marked truncation surface. There are also some internal truncation-surfaces within interval 3.1, which are generally are easier to identify as the slope steepens towards JMR.

Subinterval 3.2 is recognized by weaker amplitudes than 3.1, and more internal vertical discontinuities. At its base, reflectors are terminating into the previously mentioned truncations surface. Internally two-three additional truncation surfaces have been identified, but the dip of the internal reflectors generally remains the same. The thickness of 3.2 varies greatly depending on the depth-variations of its upper and lower truncation-surface boundaries. Both interval 3.1 and 3.2 are affected by a vertical shift at the base of the slope. This shift is different from the other discontinuities in the sections, as it is the reflections closer to the ridge that are shifted down.

Sub-interval 3.3 is separated from 3.2 by a significant truncation surface (R6) and a general change in the seismic characteristics. The seismic above R6 has a smoother appearance than the underlying layers, and in the basinal areas it is disturbed by numerous vertical discontinuities. The reflections in the interval terminate towards the slopes on either side of the JMR. R4, described in the eastern section is visible here as well, but is terminated against R6 when R6 reaches shallower levels. On top of the JMR a very clear truncation surface is visible. Due to observations on other seismic lines and the similar smooth appearance of the overlying reflectors this is also marked as R6. The upper limit of interval 3.3 is the sea floor. Downslope towards the JMB in the west, several large offset steep discontinuities dipping towards the west can be observed. A very high amplitude reflector just east of the R1 reflection stands out, and there seems to be a doming shape to the reflections above. Little is seen below the reflector.

In between and below the high amplitude reflector and R1 a series of quite clear reflections are seen, but these disappear below each of the high amplitude reflections. Directly below R1 some high amplitude reflections with an upward bend may be observed.

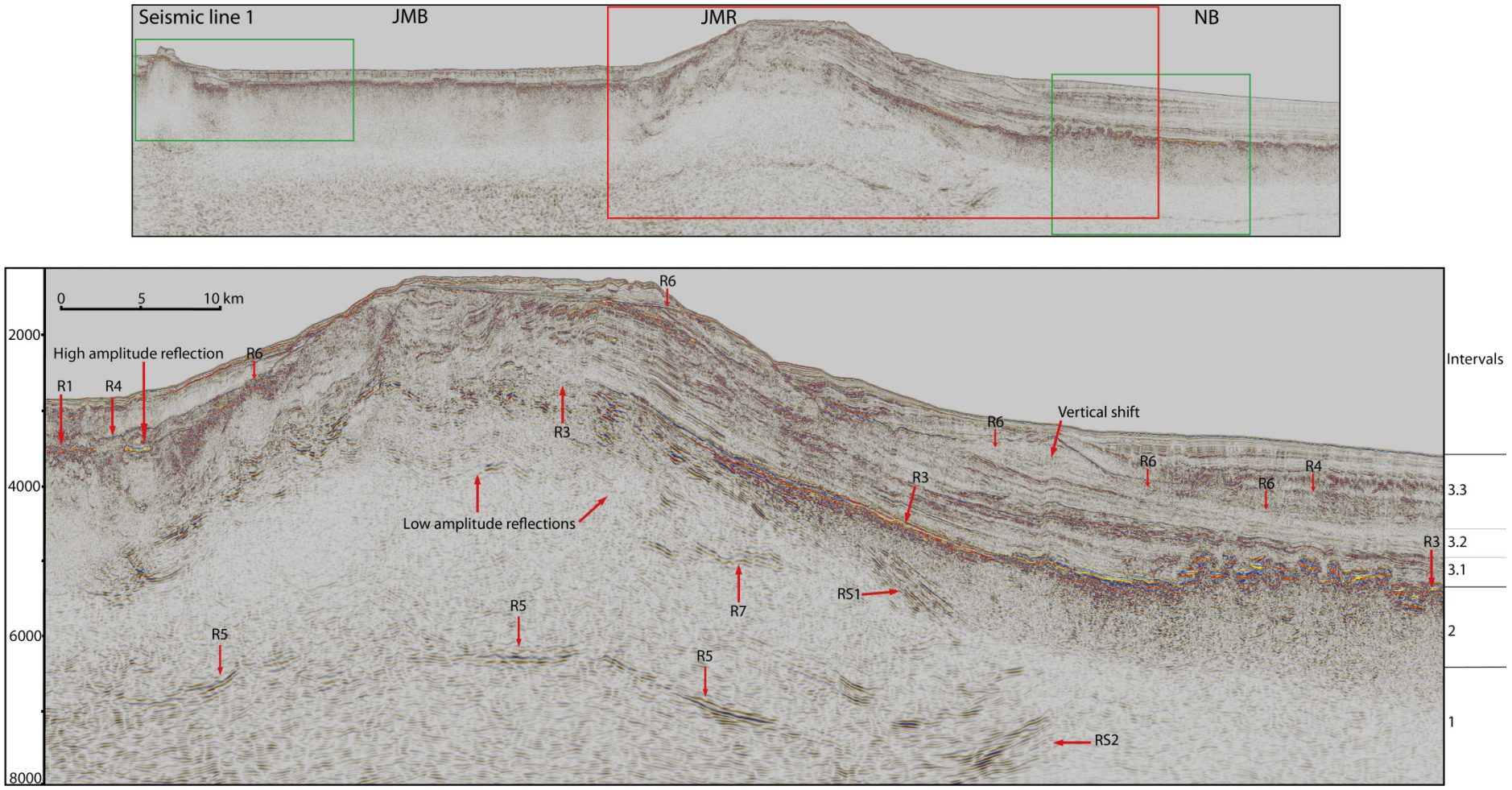

Figure 13. The middle section from seismic line 1, see text for information regarding the markings. Upper image displays the extract displayed from seismic line 1. Main observations are the seaward dipping reflectors RS1, the coherent eastern slope and the discontinuous western slope. Also note the deep R5 and RS2 reflections.R6 is present on the top and both sides of the JMR, and it truncates the reflections below.

Interpretation of Seismic line 1

From the initial observations made, and together with adjacent seismic lines an interpretation of the data has been made see Figure 14. The middle section takes in the most of the important features of the line, and has therefore been interpreted thoroughly. It is also a line that represents well the features of the JMR in the northern part of the JMMC. Compared to other seismic lines going over the JMR, it also displays more information in interval 1 and 2 like the clear RS1 features and the R5 reflector.

At the deeper parts of the line, the seismic contains very little reflections and generally displays a low amplitude, low frequency signature. While the signature could be due to a strong reflector further up masking the seismic below, the presence of the deep R5 reflector proves that reflections can make it up from the area. It is therefore likely that the signature is due to a rockfacis with little internal contrasts in impedance or a very inhomogeneous structure, as is typically within crystalline continental basement rocks. It is therefore interpreted to be crystalline basement, displayed as gray and darker gray in Figure 14. The R5 reflector displays a transition of some kind within the basement, strong enough to give a reflection from an otherwise blank depth.

The wedge-formed reflections of RS1 may be a result of two processes; either there is a marked unconformity at their top, and the strongly dipping layers underneath are terminated against this. But granted the location of the reflectors at the transition from continental crust to oceanic crust, another alternative is also possible; a volcanic seaward dipping sequence. As the acoustic impedance of basalt is expected to be higher than sedimentary rock types, the high amplitude of the R3 reflector at the top of the seaward dipping sequence supports this interpretation. The wedge-formed reflections have been extrapolated out in Figure 14 and colored red. The interpreted area should be considered with care, as the dipping reflectors are only clearly visible in a limited area.

The RS2 reflections at the base of the SDR are peculiar as they display an opposite dip from what is seen in the surrounding seismic. Gunnarsson et al. (1989) interpreted a similar type of reflections at a similar area as volcanic sill intrusions. This interpretation may also be true here if taking the RS2s close proximity to the COB of a volcanic margin into consideration. Weather the sills were intruded at the time of the SDRs or later cannot be determined. Another possible interpretation of RS2 could be a deep rotated fault block. Such a fault block would actually be expected along the continental margin even though none are visible in the seismic data. Still, the hypothesis of intruded sills seems more likely as the fault block would be very deep. Also, the varying dip of the reflections is contradictory to the fault block theory.

The green and dark orange intervals in Figure 14 are the low amplitude reflections beneath R3. Due to the large amount of reflections compared to the underlying basement and theit stratigraphic position below R3, they are interpreted as sedimentary sequences predating the volcanic SDR-sequence. The exact location of the termination of the sequences below the SDR is uncertain, and only loosely based on the data. It is however certain that they do terminate at some point as the continental crust transacts to oceanic crust given that they

predate the volcanic sequence connected to the breakup.
The sedimentary sequence above is divided into three main segments. They are all deposited later than the early Eocene breakup, as they are continuous from the continental JMR to the oceanic crust in the east.
The lower light orange colored interval and the lower part of the light green interval displays a similar dip suggesting that they have undergone most of the same uplift and/or subsidence processes. There are however several discontinuities, interpreted as normal faults, in the orange interval that terminate when meeting the unconformity that separates the two intervals. This suggests that the orange layer underwent some extensional processes before the deposition of the light green package. The orange interval is thinning towards west, but like on the eastern slope it is reasonable to assume that the unconformity at top represents an erosional surface indication that the original thickness of the layer was larger. Clear truncations of orange interval reflections seen at the location where the thickness of the orange interval is halved at the top of the ridge are trustworthy indications of an erosional event.
Both intervals are thinning towards the east away from the JMR without any clear erosive features at their top, suggesting that the sedimentation came from the west.
On the western slope of the JMR both intervals, as well as the underlying sequences are affected by the large west-dipping faults. Even though data is unclear in the basement rocks, it is reasonable to assume that the faults continue down into the basement, as the vertical displacement of the JMR into the JMB is so large.
At the base of the eastern slope the vertical shift where the landward side was is shifted down is interpreted as a reverse fault, indicating a compressional event. The fault is terminated upon reaching the yellow interval at the top.
The irregular part of R3 at the base of the eastern slope is interpreted as volcanic intrusions. This interpretation is supported by their high amplitude reflections, their abrupt terminations and their inhomogeneous structure. In addition, the observation of relatively undisturbed reflections similar to the reflections seen elsewhere in the orange interval in between the high amplitude reflections, indicate that they were deposited after the orange interval. Another feature which is typical for intrusions is the doming of the overlying reflections. Whether the doming is due to uplift from the intruded material or later differential compaction is hard to distinguish, but it no longer seems to affect the reflectors in the upper part of the green interval. The intrusion also efficiently masks the seismic below, probably due to the high impedance contrasts and the inhomogeneity of the intrusions. The top of the green interval is marked by a very clear unconformity which display clear erosive markers on the JMR slopes, and especially at the ridge top where is visible as an almost straight line truncating any underlying layers. The layers in the yellow interval onlap the unconformity along the ridge slopes, and none of the major faults beneath cross the yellow-green boundary. This suggests that the interval was deposited after the main tectonic activity in the area.

The hard R4 reflection that behaves independently of the general structural trends is interpreted to be a mineral transition few other alternatives seems realistic

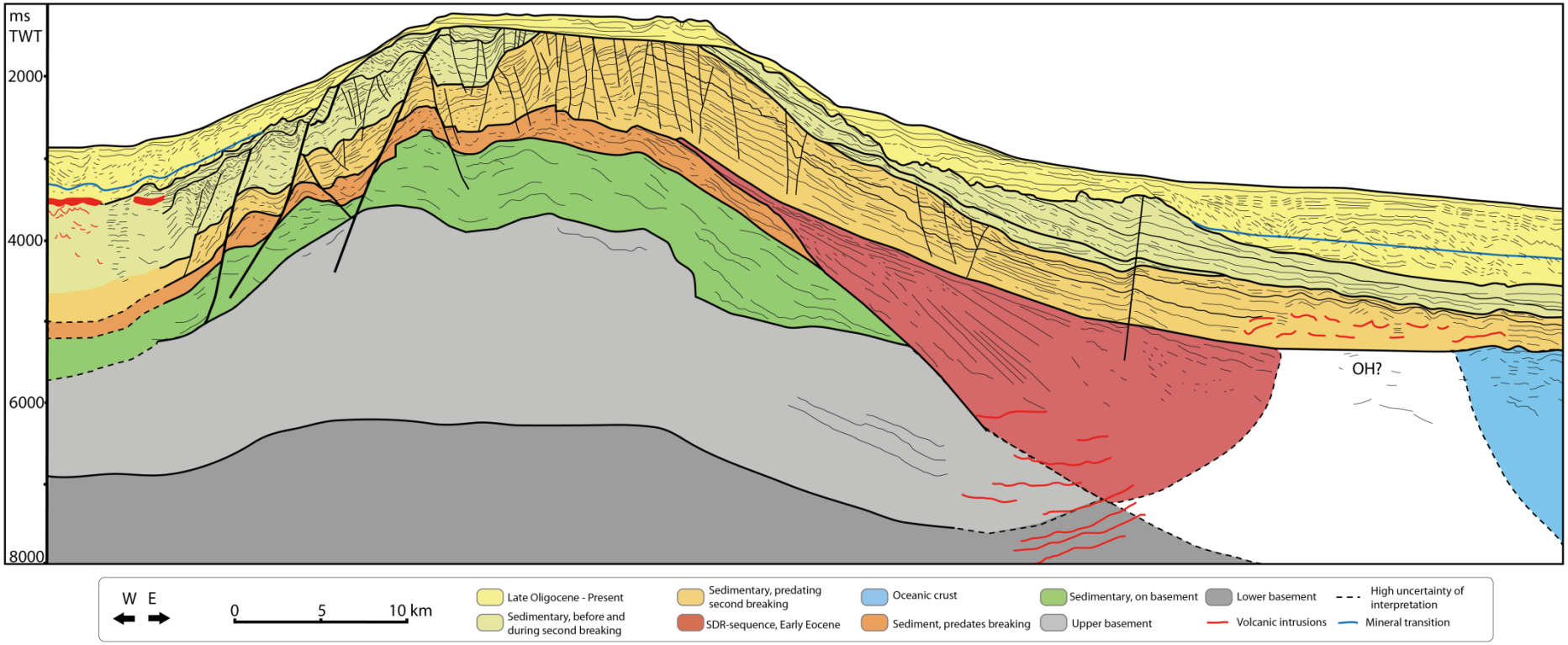

Figure 14. An interpretation of seismic line 1, middle section. Each color represents a volcanic or sedimentary sequence. The white area marked with OH (outer high) is unclear on seismic, and is where it would be expected to see an outer high based on Plankes volcanostratigraphy. Continuous black lines represent unconformities. See text in previous section for detailed description of the different interpretations.

Seismic line 2 JM-11-12

Seismic line 2 is shot over the north-eastern part of the JMB, where R1, described in seismic line 1, is not present, providing a valuable view into the structure of the JMB. The initial observations made are two positive bathymetrical features, the JMR in the east, and a smaller ridge in the JMB to the west.

At 3.2 s TWT a very strong reflection R8 is located to the west of the smaller ridge. Directly beneath it, some strong, slightly incoherent reflections are visible, but below about 3,8 s the seismic appears highly chaotic, with little or none information to be interpreted. Directly above, reflections of the overlying interval are terminating into the top of the bright reflectors

At the base of the JMB, at a depth varying between 5 s to 3.7 s a segment of high amplitude reflections are visible, (1). They appear as a series of spikes as a result of significant near vertical discontinuities. Internally, the spikes have reflections, most of which are dipping towards the west with some exceptions to the east and at the base of the western ridge. The general dip direction of reflections internally in each spike is quite consistent.

Overlying the sequence of high amplitude reflections, there is an interval (2) with a weaker seismic signal. Along the flank of the western ridge internal reflections of the interval are clear, with an increasing dip towards the east moving up towards the ridge peak. In the JMB, the interval has a varying thickness, depending on two factors; the topography of the underlying interval, and the presence of a truncation surface which constitutes its upper limit. The general dip direction of interval 2s internal reflections is varying, often the dip and vertical discontinuities are similar to those observed in underneath interval 1. In most cases though, the dip appears to be slightly gentler.

Interval 2 is separated from the overlying interval 3 by a significant truncation surface. Reflections both above and below terminate upon reaching the surface. The surface is clearly affected by the underlying intervals, as it in most cases gets deeper in between the spikes and shallower above the spikes. This is especially true where the largest vertical shifts takes place underneath. The internal reflections of interval 3 are generally horizontal, but dip upwards before they are terminated towards the underlying truncation surface. The reflections are coherent, with some vertical discontinuities on the flank of the western ridge. The appearance of the seismic is smoother than what is seen in the underlying intervals.

The boundary between interval 3 and 4 is yet another truncation surface, and it marks a transition in the seismic appearance to even smoother reflections than interval 3. The lower part of interval 4 is recognized by low amplitude, blank expression and relatively few reflections. In the upper part the amplitudes are stronger, and reflections are more abundant. The whole interval is shifted by numerous vertical discontinuities. While most of these discontinuities are restricted to the upper part of the interval, some of them continue further down until they dissipate in interval 3. As you go further up in the interval, the influence of the topography of the underlying intervals decreases. The upper and lower parts of the interval are separated by a significant hard event that appears to cut through the surrounding reflections. It is not entirely independent on its surroundings however, as it is

shifted upwards above some of the highs in the lower intervals.
To the east, the flank of the JMR is marked by a series of significant discontinuities dipping towards the west and a general decrease in relative amplitude of the seismic reflectors compared to the JMB.
The western ridge is marked by a significant near-vertical shift with a slight dip towards the east. While the reflections of interval 1, 2, 3 and lower interval 4 are clearly dipping up towards this discontinuity, the upper part of interval 4 is near horizontal when approaching the discontinuity.

At a time-depth of about 6 s there is a weak, but still clear low amplitude reflector, similar to R5 seen in seismic line 1. The surrounding seismic is chaotic with low amplitudes. The reflection is not continuous, but rather put together by several segments visible at approximately the same time-depth. It does not appear to be affected by the numerous discontinuities in interval 1 above.

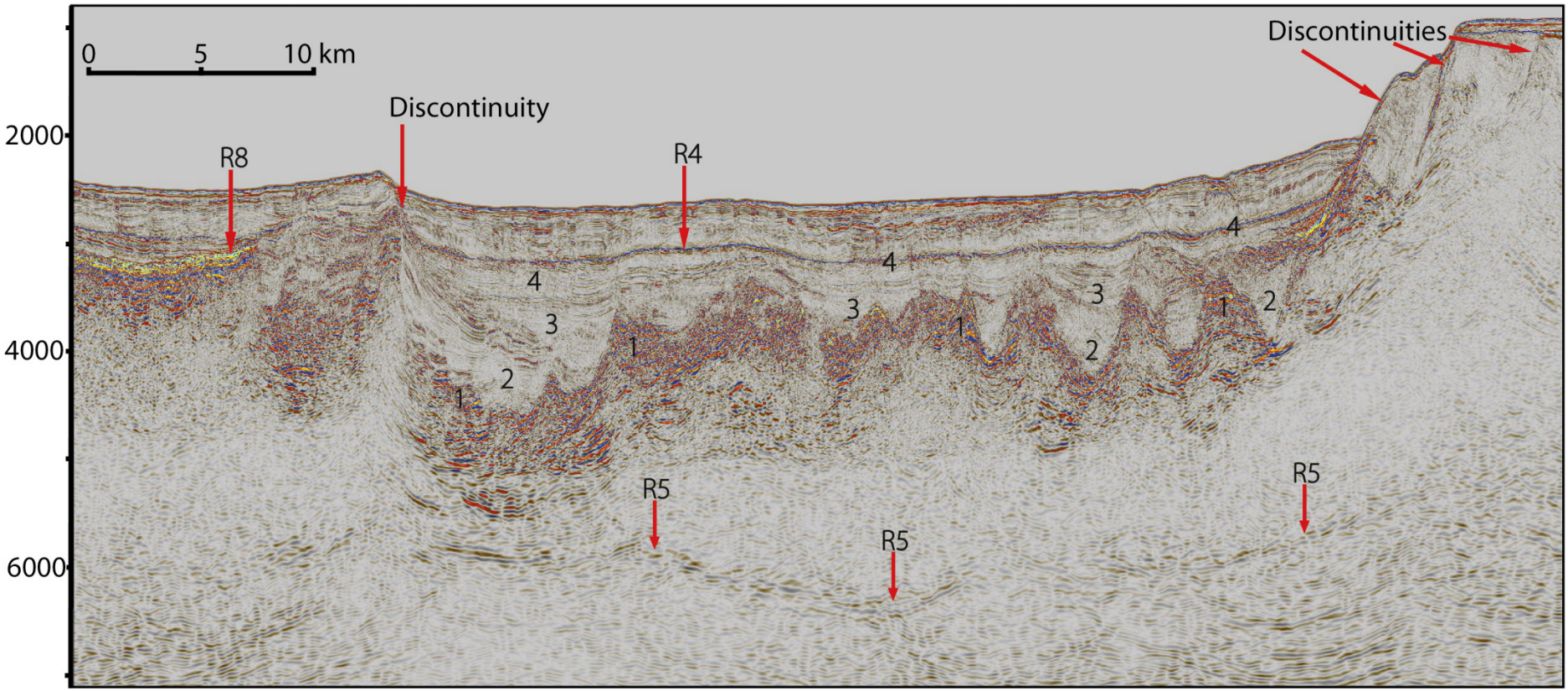

Figure 15 Seismic line 2, see text for full description of the numbering. Important observations are; the numerous discontinuities in the JMB, four intervals bound by truncation surfaces (1,2,3,4), the strong R8 reflection which terminates above lying reflections, the deep R5 reflection which does not seem to be affected by the discontinuities in interval 1.

Interpretation of Seismic Line 2

Seismic line 2 was interpreted from the observed data, see Figure 16. The interpretation of the line was complicated as a result of the heavily faulted structure of the Jan Mayen Basin. As was seen in seismic line 1 further south, the transition from the JMR into the JMB is through a series of westerly dipping faults with large displacements. The lower ridge to the west in the line appears to be a horst structure based on a large offset easterly dipping fault. The ridge also continues further south in the JMB, and creates a window where the R1 reflector is not visible. The basin between the ridges is marked by a series of faults creating horst and half-graben structures. The intervals within these structures are interpreted to be the sedimentary rocks that predated the breakup between Greenland and Jan Mayen, as the extension and rifting related to that breakup is the probable cause of the heavy faulting. The light green overlying the fault structures is clearly postdating the most severe faulting as it appears to have filled in the structures created by the faults. It is however still affected by the faults to some degree, and it is therefore reasonable to assume that the interval has been deposited syn-rifting. Reflections in interval 3 in Figure 15 are clearly unconformably onlapping the top of the light green layer. For the most part this interval is unmarked by the faults, and it is therefore interpreted as being deposited post-rifting or at least in the very last parts of the process. All the above layers are clearly deposited post-rifting.

The R8 reflection is, due to its very high amplitude reflections and the way it masks the seismic below, interpreted to be a volcanic basalt layer. As reflectors above in the yellow post-rifting interval appear to be onlapping the reflector at both ends of the reflections it is interpreted to be a extrusive basalt layer. If it was intrusive, it would not be expected to see layers onlapping the top of the reflector as the reflections above would most likely be shifted upwards by the intruded material. R8 continues further west, and is continuous with the top basement reflector of the Iceland Plateau suggesting that it is a part of the oceanic crust, and it is therefore colored blue underneath.

The R5 reflection at the base of the seismic line is interpreted to be the same reflection as was seen at the base of seismic line 1; an intra-basement transition. It is however hard to interpret the upper boundary of the upper basement, it is therefore represented as a gradual transition from gray to green in Figure 16. That the top of the basement is hard to identify on the seismic could be caused by high acoustic impedance in the overlying sedimentary rock types which may be caused by cementation or high degree of compaction. A high acoustic impedance in the sediments would create a low contrast at the sediment-basement transition. This is supported by the high amplitude reflections seen in the orange layer. These strong reflectors would also mask the signal from underlying reflections.

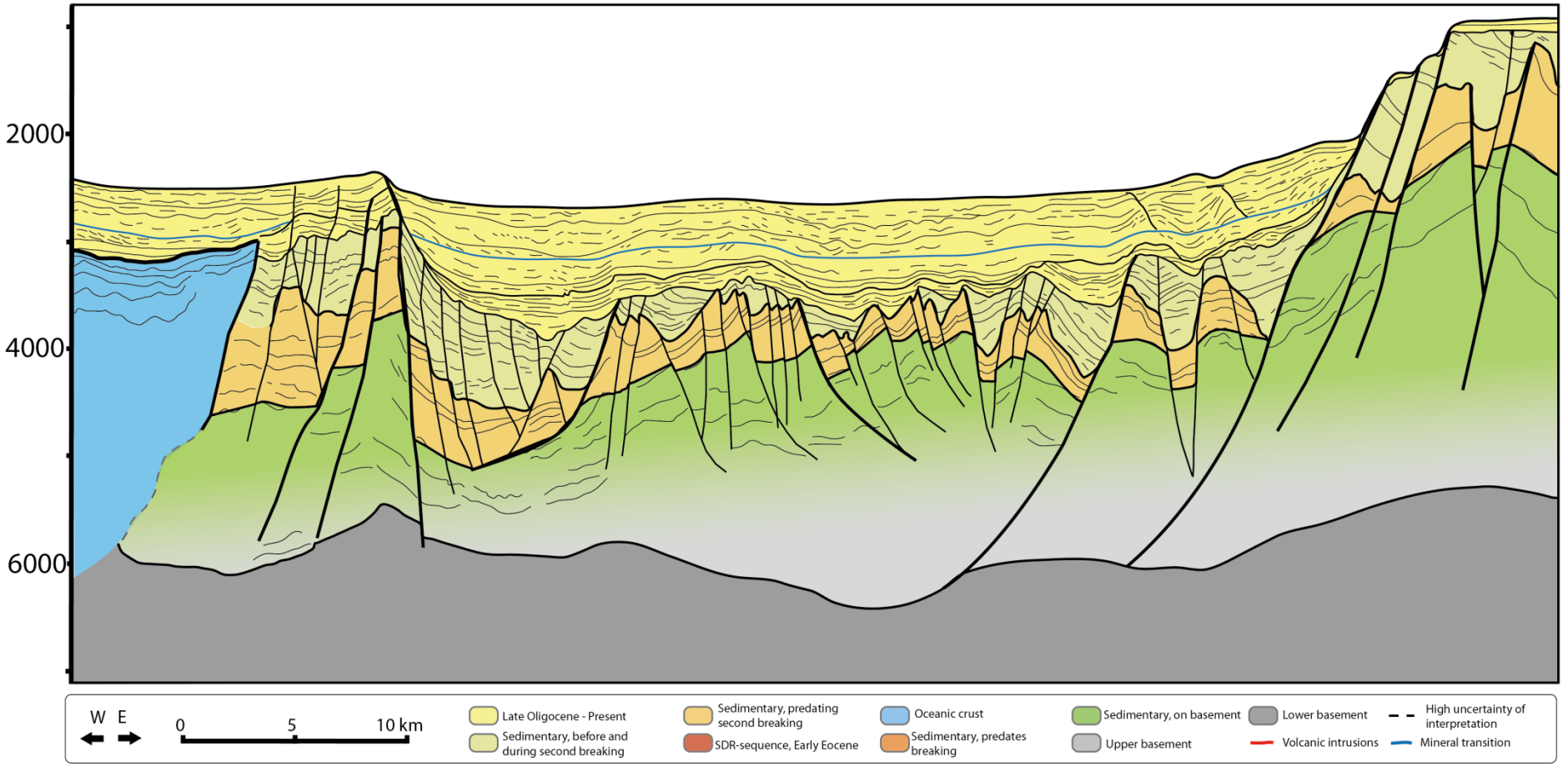

Figure 16. Interpretation of seismic line 2. See text for full explanation.

Seismic Line 3, JM-11-01

Seismic line 3 is the southernmost east-west trending seismic line in the data set. The main features of the line are four structural highs, two of which stands more than 1 s above the surrounding sea bottom topography. The line is for practical reasons cut into two images, the eastern Figure 17, and the western Figure 18.

The easternmost ridge is characterized by a very steep slope (averaging 34 degrees) dipping towards the west, and a gentler slope (averaging 12.2 degrees) dipping towards the east. Internally, the ridge has a series of reflections dipping to the east that terminate against the steep slope in the west. The whole section starting from the steep west slope and to the end of the line in the east is similar to what is seen along the JMR further north. At the base of the line, the seismic is highly chaotic, with little detail visible. From about 5.5 s TWT a series of low amplitude, seaward dipping reflectors are visible at the base and the lower part of the slope. The reflections terminate towards a high amplitude reflection, R3, which may be followed from the top of the slope and all the way to the east. The amplitude of R3 increases towards the bottom of the slope and even further east. From the bottom of the slope and eastwards R3 changes significantly. Close to the slope, it is fairly high amplitude with coherent reflections except for a few vertical discontinuities. About 11 km from the slope, the reflector is disturbed and no longer visible due to the presence of some very high amplitude reflections above the depth at which R3 was visible. The reflections are highly irregular in shape and are divided into several segments which are present at depths varying between 4.3 s and 3.8 s. Very little details is visible below these reflections, but close to and in between the segments, reflections with similar dip and seismic signature to the interval above are present. The whole zone of disturbed reflectors is about 17 km long.
Further east R3 changes its signature again to a smooth top reflector, with an interval of high amplitude chaotic reflectors below. A 10 km wide segment of the reflector has a broad mound-shape, and the underlying high amplitude sequence seems to follow the dip of the mound.
Above R3 there is an interval of lower amplitude reflectors. East of the slope the reflections are heavily influenced by small scale discontinuities, but if these are disregarded, the reflections are quite coherent. The interval is divided into three sub-intervals based on their seismic signature. The boundaries between the intervals are major lines of reflection-truncations. The lower interval has relatively low amplitudes, and its lower part is recognized by having few clear reflectors. Its upper part has clear reflectors, especially up the slope of the ridge. Two of these reflectors are clearly truncating the surrounding reflections. The middle interval has higher amplitudes than the lower interval, especially on the slope. Its upper part has a smoother appearance than the lower part. There are two clear lines truncating the surrounding layers within the interval seen all the way from the slope to the eastern part of the seismic section. The upper sub-interval may be recognized by a smooth appearance of the seismic, and numerous discontinuities fragment the reflections. The dip of the reflections varies in a wave-like manner towards as you move towards the east from the

slope. The upper part of the interval both the smoothest, as well as the part that is suffering from the most fragmentation by discontinuities. Through the middle of the interval, a significant high amplitude hard event is crosscutting the dip of the surrounding reflections, R4.

The area between the eastern ridge and the JMR, the JMT, is dominated by a strong hard event, R1, at about 3.3 s TWT. It consists of three segments that are separated vertically by about 100 ms.
The seismic below the reflector is highly chaotic with no clear reflectors. The exception is a found at the base of the steep slope of the eastern ridge, where R1 is absent. There it is possible to see a deeper interval of near-horizontal reflections. They are mostly high amplitude events, and some appear to truncate the others. The interval from R1 to the sea floor is divided in two sub-intervals. The lower is quite chaotic and it is hard to find and follow any coherent reflections. The upper part is smoother with consistent reflectors, and is thicker towards the western part of the JMT. The whole interval is heavily affected by numerous near-vertical discontinuities.

The JMR has a distinct appearance this far south. Its width is reduced compared to further north, and the slopes on either side are very steep, about 30 degrees, with a vertical elevation of 2000 m. The sides appear to be discontinuities continuing far down into the underlying seismic. It is dominated by one strong blue reflector, R4. Reflections above R4 are clear and smooth, while the reflectors below are low amplitude and difficult to make out.

Down the western slope of the JMR and to the first low ridge to the west there is a basin-like structure with several intervals of reflectors. At the base there is an interval where the reflectors are low frequency, and of varying clarity. Above these lower reflections there is an interval (1) of coherent reflectors dipping heavily to the east. Internally in the interval there are several discontinuities. Reflections are terminated by truncation lines on both sides of the interval.
Interval 2 above is recognized by a sequence of clear coherent reflectors in the middle of the basin-like structure. The reflections are dipping down along the slopes towards the center of the basin at a gentler angle than the underlying interval 1. Amplitudes increase in the upper part of the interval. The upper interval 3 is characterized by a smooth seismic appearance, numerous small discontinuities and a blue R4 reflector crossing the other reflections.

Between the two lower ridges and all the way to the west, the seismic is similar to what was observed in the JMT.

The western lower ridge has a steep slope to the west, associated with a deep discontinuity dipping towards the west, and a gentler slope on its eastern flank dipping to the east. On the ridge, little clear data can be observed from the seismic below time-depth of 3,8 s TWT. Above this depth a sequence of west-dipping high amplitude reflectors is observed,

disturbed by several smaller discontinuities dipping towards the east. The whole high amplitude sequence rests on a larger easterly dipping discontinuity. Further up there in an interval of medium amplitude reflections. There appears to be several lines truncation reflectors within the sequence, causing it to be quite chaotic. The interval is bounded by a clear line of truncations at the top, which marks a transition to a much smoother appearing seismic.

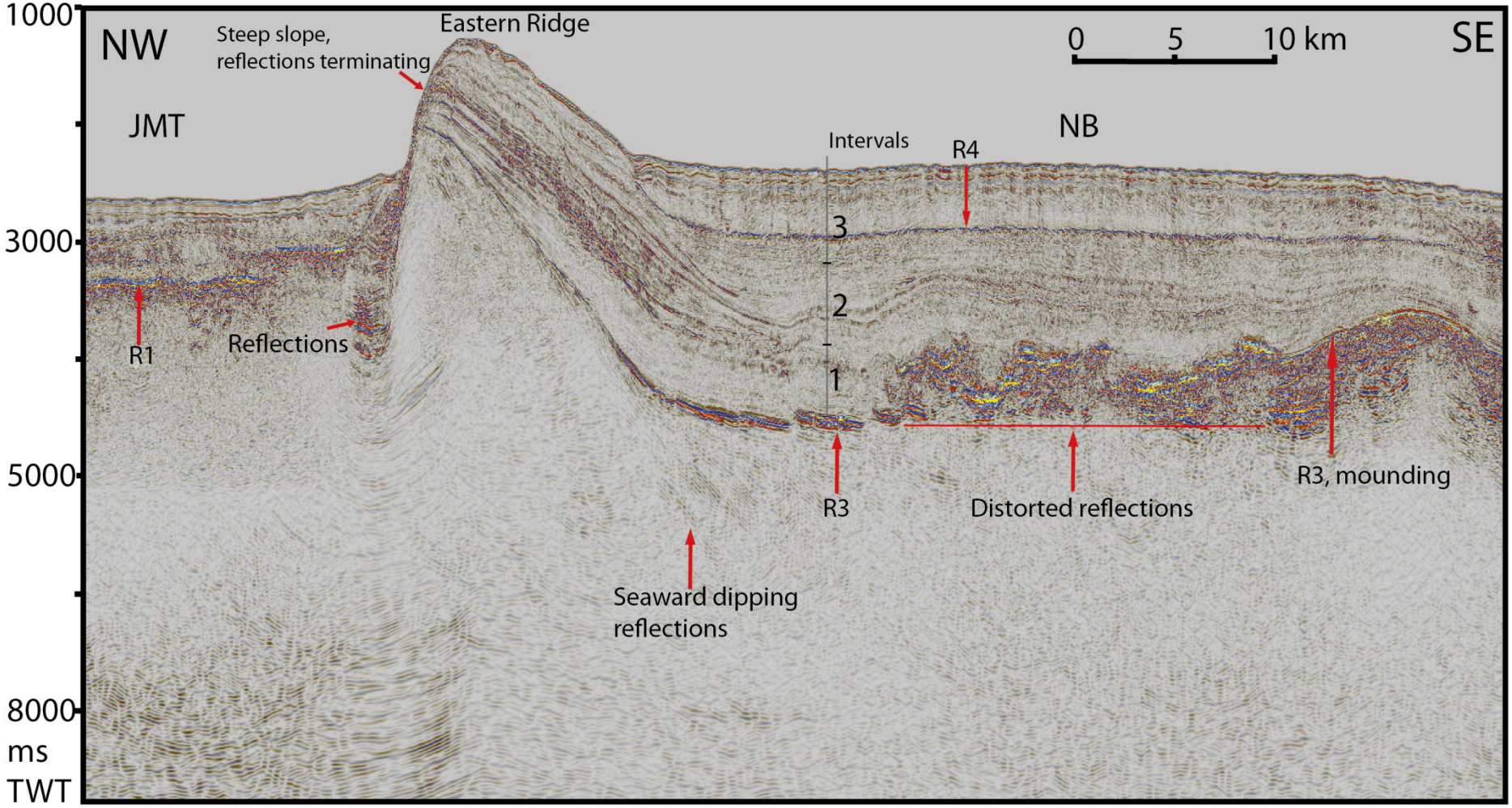

Figure 17. The eastern section of seismic line 3. Important observations are the seaward dipping reflections, the eastern ridge with a steep discontinuity, the distorted part of R3, and the intervals 1,2

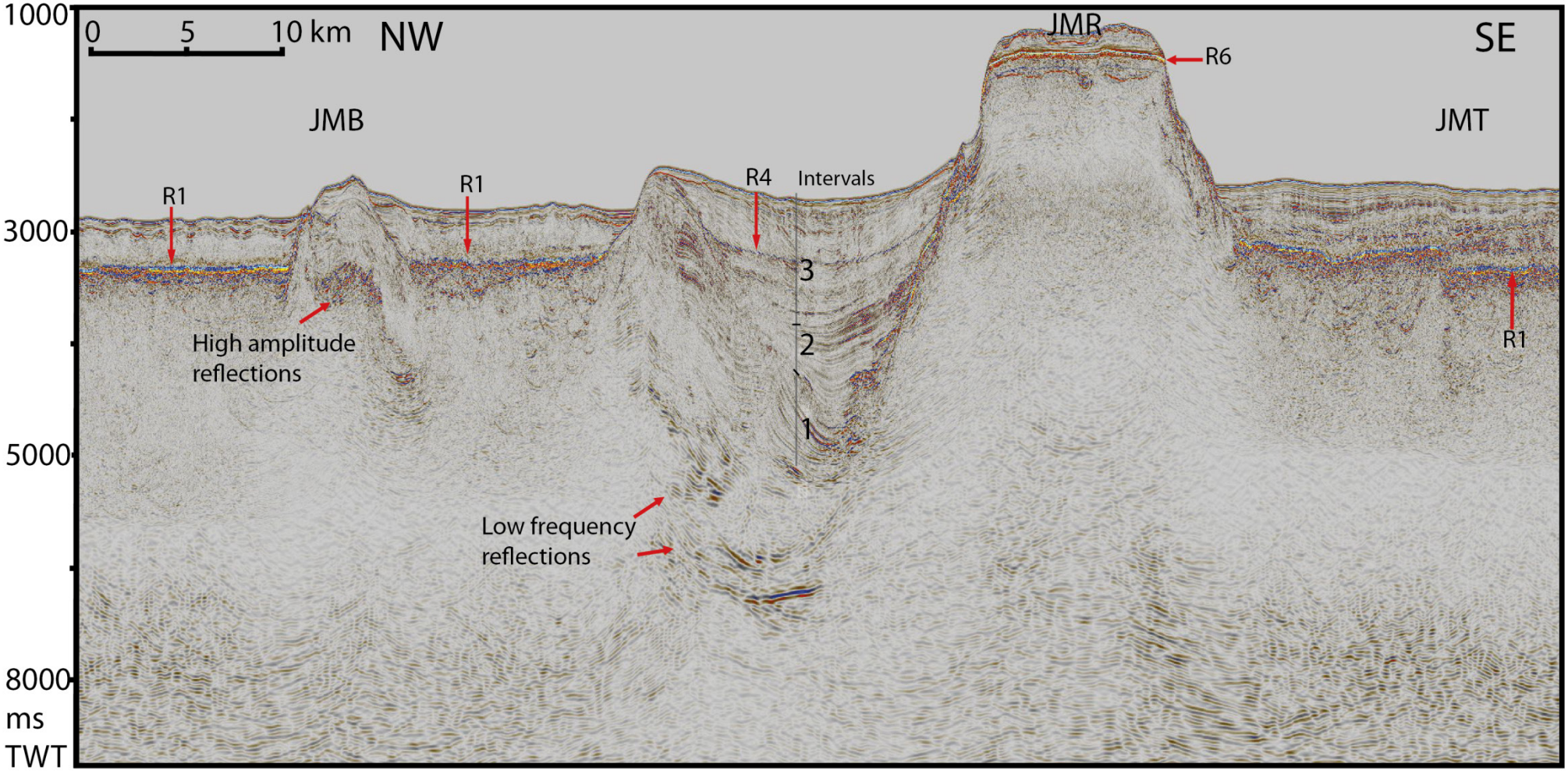

Figure 18. The western part of seismic line 3. Important observations include the extreme steep nature of the JMR and its lack of clear reflections, the presence of R1 in the JMT and the JMB, the observation of interval 1,2,3 in the structure to the west of the JMR, and the high amplitude reflections on the ridge in the JMB. It should also be noted that R1 terminates upon reaching the ridges.

Interpretation of seismic line 3

Seismic line 3s location south in the investigation area displays the differences between the southern and northern parts of the micro continent. The JMR has spilt into two separate ridges, where only the middle one is continuous with the northern ridge. The two are separated by the Jan Mayen Trough (JMT) in which the seismic is masked by the R1 reflector, same as seen in the Jan Mayen Basin to the west. The ridges are clearly a result of dramatic, steeply dipping faults, but whether or not they flatten out and become listric further down is not possible to ascertain with any certainty based on the seismic data. Correlating intervals from one ridge to the other is difficult because of the large displacement of the faults and the presence of the R1 reflector masking the areas in between the ridges. Most of the seismic data from the area are lines shot perpendicular to the strike of the faults, further complicating the process as direct seismic correlation between these lines is not possible. Most of the correlation between the different ridges is therefore based on analysis of the seismic signature of the different packages, together with the interpretation of tectonic processes associated with each time period. Key unconformities were also identified, but it should be kept in mind that the tectonic uplift and subsidence processes might have happened at different times, resulting in different unconformities.

The eastern ridge is generally quite similar to the interpretation of the JMR in seismic line 1, Figure 14. The main difference is the western flank of the ridge which is steeper in seismic line 3, and it appears that the entire displacement into the JMT is caused by one major fault, unlike the multiple faults seen towards the JMB in seismic line 1. Due to their small extent of the reflections seen at the base of the fault, the given color intervals should be used with care. This also goes for the pre-Eocene breakup interpretations on the eastern ridge. Determining the top basement proved difficult, and was therefore not included I the interpretation.

Oceanic basement is interpreted to start at the western base of the mounding of the R3 reflector. This is backed by the fact that the SDR-sequence is no longer visible at this point, and that reflections in the orange interval are observed to onlap the mound. The mounding itself is interpreted to be of volcanic origin due to its placement and the high amplitude reflections that are associated with it. A probable mechanism behind its creation is a volcano due to its large extent (~14 km wide east to west) and significant relief (~0.4 s). The internal reflections in the mound tend to be dipping down from its center along the flanks, while the center itself is more chaotic. This could correspond to a fissure in the middle, with basalt flows forming down the slopes of the volcano.

The orange interval is interpreted to have filled in the space between the mound and the slope, and it therefore significantly thinner on the top of the mound.

The bright irregular reflections in the orange interval just west of the mound are interpreted as volcanic intrusions similar to those seen in seismic line 1. Just west of the intrusions there are two near vertical faults where the landward side is shifted down, possibly reverse faults.

Whether or not the unconformity that is the boundary between the orange and the light

green interval is the same as interpreted further north proved hard to establish as there are several unconformities at similar depths. The boundary was established by examining where the faults in the lower part of the ridge sequence terminated as was seen on the western slope of seismic line 1. The unconformity that was identified also provided a significant transition from high amplitude reflectors to a lower reflectivity sequence above. The faults are nearly vertical and no antithetic faults have been identified. It is therefore suggested that the tectonic process that lead to their creation was related to the initial uplift of the ridge rather than the rifting associated with the first breakup.
The light green interval is also faulted on the high, but the angle of the faults is slightly slacker than the faults of the orange interval, and is therefore probably related to another tectonic process.
In the yellow interval above layers are clearly onlapping the slope of the top green unconformity, and are therefore interpreted to be deposited post-breakup.

Within the JMT the R1 reflector masks the seismic, but similar to other observations seen elsewhere some smile-shaped reflections are seen underneath. The smile-shape of the reflections may be a result of using too high velocities in the velocity model for the migration of the seismic data (Zhu et al., 1998). The reflections might still be real, but determining whether or not they are sedimentary or volcanic in origin is not possible with the current data. One possibility is that they are volcanic sills or dikes, which would explain that their reflections are strong enough to be seen below the R1 reflector. Another possibility is that they are intra-bed multiples from within the R1 reflector.

Within the JMR structure very few reflectors may be seen, except the signature near horizontal erosional surface of the bottom yellow interval at its top. The lack of reflectors in the ridge could be due to a N-S structural trend where the southern end of the ridge has been shifted upwards, resulting in that the late Oligocene unconformity lies directly on pre-breaking sedimentary rocks or even basement rocks.

The basin-like feature on the western flank of the JMR is interpreted as a down faulted, rotated, fault block which has generated a half-graben structure. Judging by the dip of the interpreted sequences in the structure it appears that the orange layer was deposited before the fault activated. The orange interval is also affected by a complex series of faults which are interpreted to be the result of extension and gravitational response from the stretching of the layers that would have happen during creation of the fault block. The green and yellow intervals are interpreted to have been deposited after the main period of activity along the major faults as the dip seen in these sequences can be explained by differential compaction.

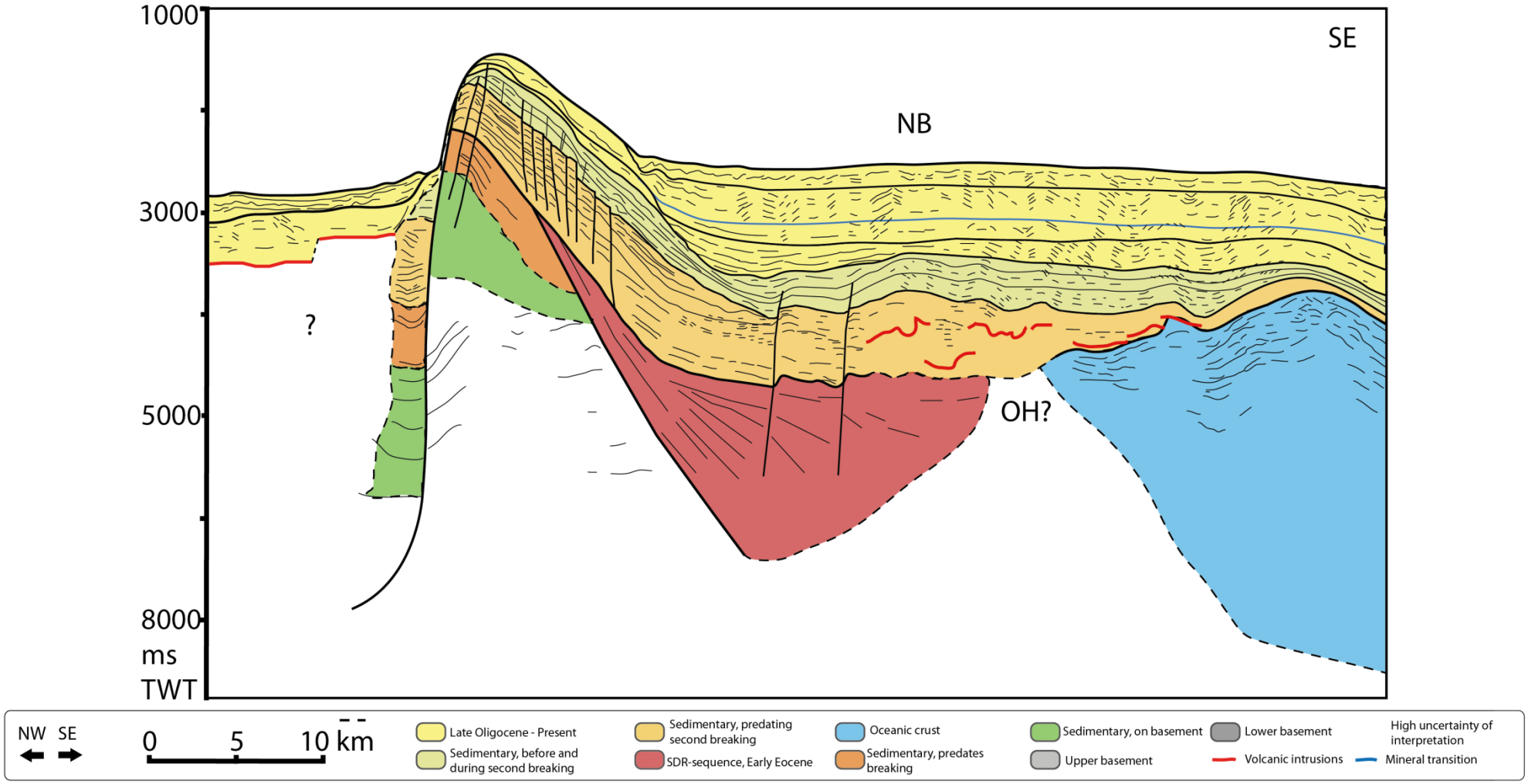

Figure 19.Interpretation of seismic line 3, eastern section. Main features is the presence of a volcanic seaward dipping sequence, a volcanic mounding interpreted as top oceanic basement, volcanic intrusions in the orange sequence, and the identification of three post-Eocene breakup sedimentary rock intervals.. NB (Norwegian Basin), OH (Outer High).

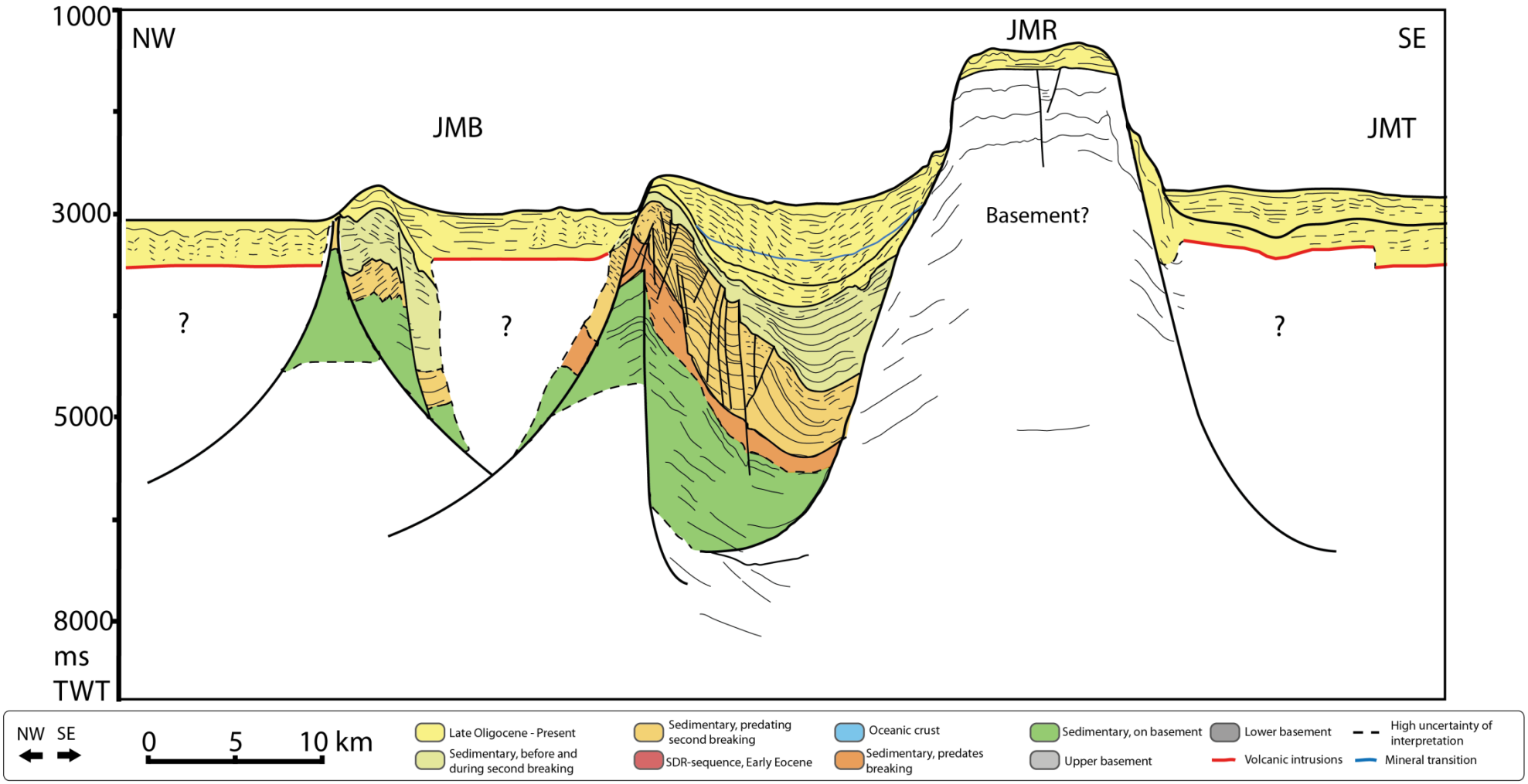

Figure 20. Interpretation of seismic line 3, western section. Important features is the volcanic R1 reflector in the Jan Mayen Trough (JMT) and the Jan Mayen Basin (JMB), the identification of sedimentary sequences in the half-graben down slope from the Jan Mayen Ridge (JMR), and the timing of these relative to the main fault activity. The apparent lack of younger sedimentary sequences on the JMR should also be noted.

Interpretation of volcanic reflectors

Having a negative impact on the efficiency of the seismic imaging, as well as being important clues to the geologic development of the Jan Mayen Micro Continent (JMMC), mapping of the volcanic reflectors R1 and R3 and the eastern and western oceanic crust is important. The extent of the SDR-sequences and the volcanic intrusions on the western slope has also been mapped. For an overview see Figure 29.

Identifying the western oceanic crust

Identifying the transition to oceanic crust based only on seismic reflection data is difficult, as the reflector of the oceanic basement can be hard to distinguish from other volcanic features, such as the R1 reflector.

A common method of identifying oceanic crust is to record magnetic anomalies. These anomalies are the results of reversals of the earth's magnetic poles. When a volcanic rock solidifies, minerals are oriented according to the orientation of the magnetic field at the time of solidification. As a result, rocks are magnetized, and this may in turn be recorded by magnetometers. Around mid ocean ridges, volcanic rocks are produced at a relatively constant rate and the magnetic polarization of the rocks may therefore be recorded as more or less parallel lines centering on the spreading center. These magnetic anomalies have been recorded and dated, giving the possibility to observe the past growth of the oceanic crust.

Peron-Pinvidic et al. (2012a) displayed such magnetic data along a seismic line, providing a link between the magnetic and seismic data. Although the same seismic line was not available in the dataset used in this thesis, a similar adjacent line (seismic line 4) was used to investigate the transition. Due to the similarities between the two it is reasonable to assume that the magnetic data may be applied with good accuracy.

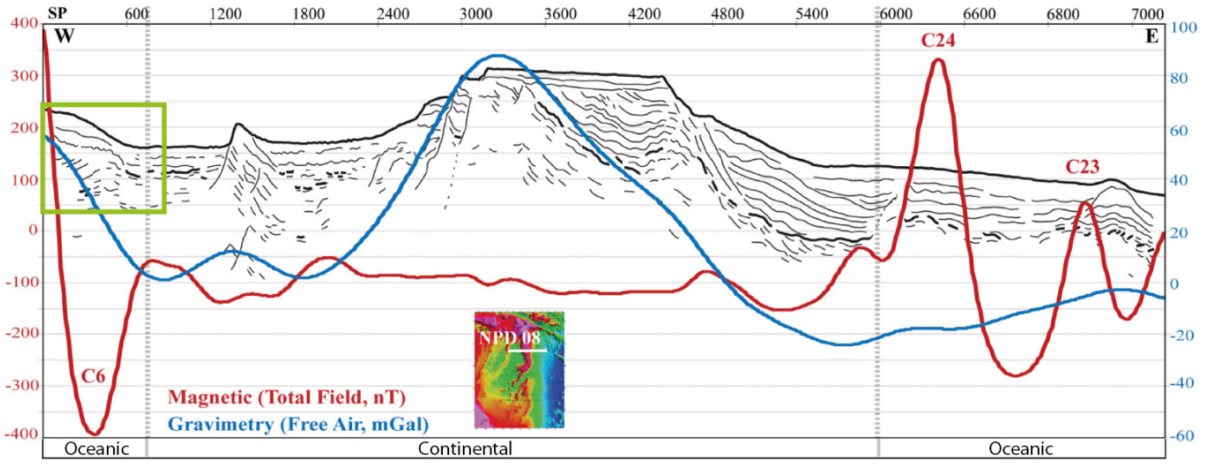

Figure 21. Magnetic and gravitational potential field measurements over the JMMC. Green rectangle indicates the western continent-ocean-transition, close to the seismic line 4. C6, C24 and C23 are magnetic anomalies associated with oceanic crust. Modified from Peron-Pinvidic et al. (2012a).

Observations from seismic line 4

The initial observation (see Figure 26) from the seismic line is a bathymetrical high rising up from the flat JMB to the east. Central on the high, at a time depth from 2,25 s to 3.3 s TWT a hard, high amplitude event is dipping towards the east, R9. To the west it terminates against a near vertical discontinuity, but continues at 3 s before continuing out of the section. The event consists of a hard top reflector, but several reflections of hard and soft events with equally high amplitude are visible directly below, and giving the event a thick appearance. This thickness is thinning towards the terminations of the reflection. Further below the seismic is chaotic until a depth of 4 s, where some low frequency reflections may be seen.

To the east of the high, the R1 reflection is visible, in two distinctly straight, horizontal segments that are offset by about 0.1 s by a vertical jump. The top reflection of R1 is weaker than R9, and it appears more unclear. It does not display the same clear repeated hard and soft events as was observed in R9, and no reflections are visible below. The low frequency events at 4 s below R9 terminate at the transition from R9 to R1.

Above R1 and R9 an interval of reflections are visible. They are dominated by numerous vertical discontinuities which together with one strong hard event that is relatively unaffected by these (R4). The interval is thicker above R9 than above R1. Just below the sea bottom on the high a thick soft reflector is visible. A similar event is visible to the east of the high. The soft event is terminated on the eastern slope of the high when the sea bottom makes an abrupt increase in depth. At the base of the slope an area of the seismic appears uneven and chaotic.

Interpretation of seismic line 4

From the magnetic field data in Figure 21 a clear magnetic anomaly, interpreted as chron C6, is present in the Seismic line 4 area, suggesting the presence of oceanic crust. Seismic line 4 includes the transition from non-polarized continental crust to the polarized oceanic crust. The R9 reflector and the bathymetrical high correspond well with the magnetic anomaly, suggesting that it is a part of the oceanic crust. Being high amplitude, hard event at a shallow stratigraphic level in the continent-ocean transitional area suggests that R9 has a volcanic origin. Further west, R9 continues only offset by what is interpreted as normal faults dipping towards the west. The lower reflections in the sedimentary interval covering the high do not appear to onlap R9, suggesting that the high was uplifted after the deposition of these sediments. Assuming that R9 is volcanic, the internal high amplitude hard and soft reflectors associated with the event could be the result of a mixture of basalt flow and sediment deposits. The high impedance basalt flows would generate a hard event on seismic while periods of lower acoustic impedance, non-volcanic sedimentary deposition could generate the soft reflections. They could also be the result of variations between the flooding events, and the internal variations between the interior and the exterior of each flow. Such basalt flows might be sourced in a sea-floor spreading environment, and together with the other data it is found very likely that R9 is the top oceanic basement reflection (see Figure 27). R9

was interpreted on seismic lines to the north and south of seismic line 4, and the extent of the reflector within the investigation area may be seen in Figure 29. The high seen in seismic line 4 may be seen along the initiation of the oceanic crust in most of the investigation area, and it is interpreted as a regional event.

The mineral transition in seismic line 4 (see Figure 27) appears to follow the bathymetry of the area and appears at roughly the same sediment depth at throughout the section, as is typical for a reaction that depends on pressure and temperature. An exception to this is the area where the soft event truncates on the slope of the high, where the transition appears to be shallower below the sea floor than elsewhere. This suggests that the thickness of the overburden used to be greater in that area. One explanation for this is that a submarine landslide has moved the most recent sediments downslope. This is supported by the presence of a chaotic area in the seismic at the base of the slope which could be the impact area of such a slide.

The R1 reflector

The R1 reflector is relatively easy to map in seismic due to the hard, high amplitude reflection and the masking of the underlying seismic that is associated with the reflector. These seismic properties are the main arguments for interpreting R1 as being of volcanic origin. The thickness of the sedimentary interval above the R1 and R9 reflections may say something about the timing of the events. If the R9 reflection event is interpreted to be basalt floods it is inferred that they were extrusive on the paleo-surface, either submarine or sub-aerial. As the flood and sea-floor spreading happened adjacent to the JMB it is likely that the paleo-surface was also continuous from oceanic to continental crust. Since the uplift of the marginal high is interpreted to have happened after some of the sedimentation on top of R9 happened it is therefore likely that these sedimentary layers should also be found in the JMB. They are however not observed above the R1 reflection in seismic line 4. One possibility is that the R4 mineral transition reflection masks the reflections in seismic line 4, but when observing other seismic lines (see Figure 23) it appears as if the sedimentary layers continue below the R1 reflection. This indicates that the R1 reflection is deposited after the oceanic basement R9 reflector.

Determining what kind of volcanic deposit R1 is proved difficult. Possible emplacement processes could be sub-aerial floods, submarine floods, volcanic ash (Peron-Pinvidic et al., 2012a) or intrusions. As R1 was deposited after the rifting associated with the Early Miocene breaking the area was so low that it was probably deep below sea level. This would rule out sub-aerial floods.
R1 was mapped over most of the Jan Mayen Basin area, approximately 7000 km^2, and there is no southward limit within the investigation area of this thesis (see Figure 29). It is also present in the Jan Mayen Trough area, adding around 1500 km^2. The reflection appears to follow the bathymetry, terminating towards the highs in the area. This would most likely eliminate the ash option; as such an event would be expected to be seen across the entire

area, regardless of the topography. A tuff would also not be likely to cause the masking effect of the underlying seismic, as the impedance contrast between sedimentary rocks and tuffs is relatively small.

So, similar to Peron-Pinvidic et al. (2012a), it is found that the most likely mechanisms behind the reflection is either submarine flows or intrusions. Holcomb et al., 1988, as summarized by Planke et al. (2000) found that submarine lava flows may flow for at least 100 km in lava tubes, indication that the distances in the JMB could indeed be covered by underwater flows. It would be expected that such a large area could not be covered in one single flow, leaving time for sedimentation in between the volcanic flows as interpreted for the R9 event, but the two reflectors are instead quite unlike, suggesting different emplacement processes.

A major irregularity identified on the R1 reflector is the abrupt vertical shifts which divides it into segments. These could be formed by steep normal faults postdating deposition of the vulcanite, but in some cases the displacement between the segments seems larger than the observed changes in the sediments above. While this could be caused by that the faults were active shortly after R1s emplacement, it should be noted that such irregular behavior is commonly seen among intrusives. The abrupt terminations of the reflector are another feature of intrusions. The topographic control on R1 could be a result of changing pressure conditions from the basin and onto the highs. The compressional forces that must be overcome in order to induce a fracture where the intrusion can propagate could be higher towards the high, effectively stopping the intrusives from intruding into the ridge areas. This hypothesis is also mentioned by Peron-Pinvidic et al. (2012a), but it represents a significant aspect of uncertainty to an intrusion-interpretation.

Below the R1 reflector, very few other reliable reflections are visible. The exception is the presence of bow-shaped reflections (see a well-developed example in Figure 24). These are not visible to the same extent as R1 itself, but do occur commonly throughout the JMB. They as best developed along the areas where R1 terminates against the topography. The bow shape of the reflections could be due to bad migration during processing of the seismic data. Some of the reflectors seem to be repeated downwards indication intra-bed multiples, but a fair amount of them appear unique in shape. If the reflections are real and not just effects of the data processing or multiples, they must be high amplitude events in order to be the only data imaged below R1. They have therefore been interpreted as volcanic sills and dikes within the sedimentary rocks in the JMB. If this interpretation is valid, it supports an intrusive model for the R1 reflector by saying that there could be a source for the volcanic material directly below rather than another distant source. This does however not rule out the submarine flow model, as the flows too could be sourced by the same process as it emerges on the paleo-surface.

A final input for the interpretation is a high amplitude reflector present in the part of the JMB which is not covered by the R1 reflector, see Figure 25. The reflection is located below the R1 in the stratigraphy, and is due to its very high reflection response compared to the surrounding seismic interpreted as an intrusion. Towards the edges it displays an upward

dip, and then flattening, suggesting that it is a saucer-shaped type intrusion. This is supported by the doming of the overlying reflections. It should be noted that the observation is from the poorly migrated 2012-data, which should be considered when observing the reflection. Using the relationship found by Polteau et al. (2008b), where the inner sill of a saucer shaped intrusion is 4-5 times as wide as the overburden is thick, an estimate of the deposition depth of the intrusion can be made. The inner sill is measured to be 3235 m, suggesting that the overburden would have been between around 800-650 m. These numbers are only approximate, as the exact width of the inner sill is difficult to judge from seismic. However, if using an approximate seismic velocity of 2000 m/s for the overlying sediments, it implies that the paleo-surface was positioned at 800-650 ms TWT above where the intrusion is located today, assuming that the sedimentary layers above are comformable. The intrusions inner sill is located at 3800 ms TWT in the seismic line. If the calculations are approximately correct this would put the paleo-surface at a time-depth of around 3000-3150 ms. This is well above the stratigraphic level of the R1 reflector, which is commonly occurring at about 3500 ms TWT.
If the two volcanic features are related to the same process, such as an increase in the mantle temperature and melt production, and were emplaced at roughly the same time, it would imply that the R1 reflector would be deposited below the surface as an intrusion.

Due to the many assumptions in this calculation, it should only be considered as uncertain at best. A more secure implication of the intrusion is that it demonstrates that it is possible for intrusions to be generated from what is likely a local source in the JMB.

While nothing definite may be said about the emplacement process behind R1 and intrusions in the JMB, it is indicated from the observations that it is likely either a submarine basalt flow, or a volcanic sill intrusion. Based on the evidence seen in this thesis, it is interpreted as the latter of the two.

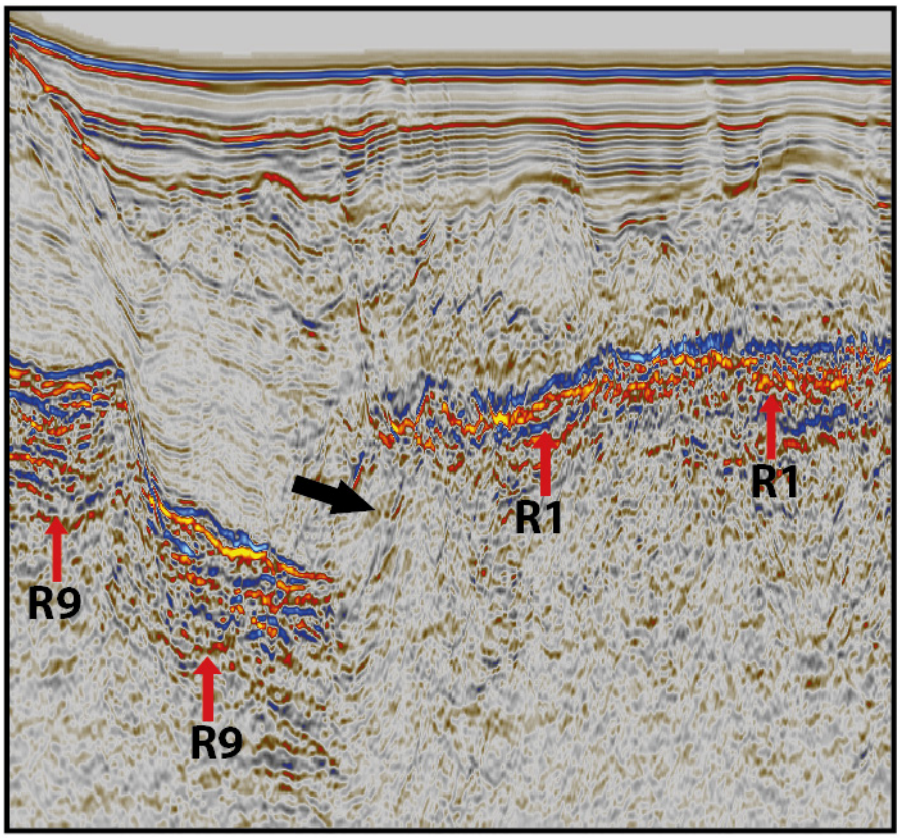

Figure 23. Observe how sedimentary layers present on the oceanic crustal high to the west probably continues down below R1 in the direction indicated by the arrow, indicating that R1 postdates R9.

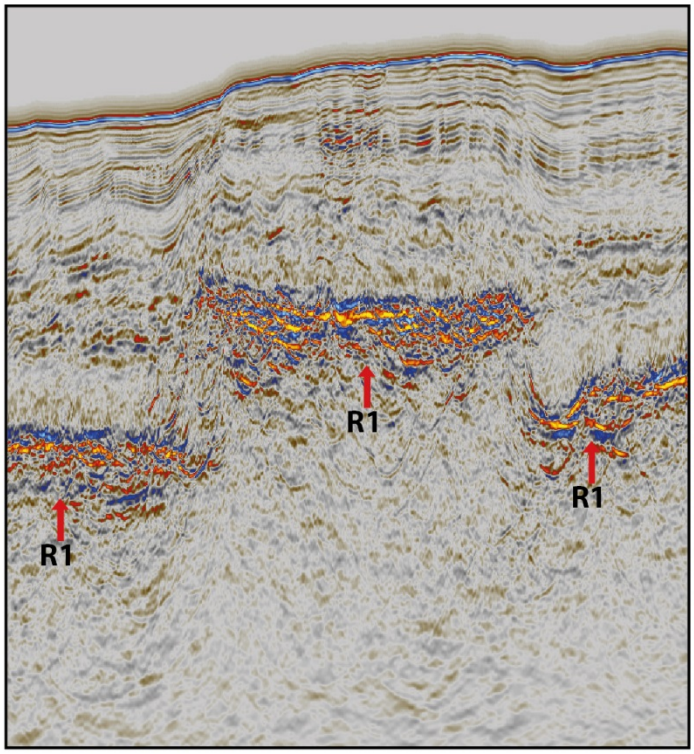

Figure 22. Example of a significant vertical shift of R1. Notice how the sedimentary column above R1 decreases above the uplifted section. The shift is about 400 ms TWT, and the uplifted section is about 4.5 km wide.

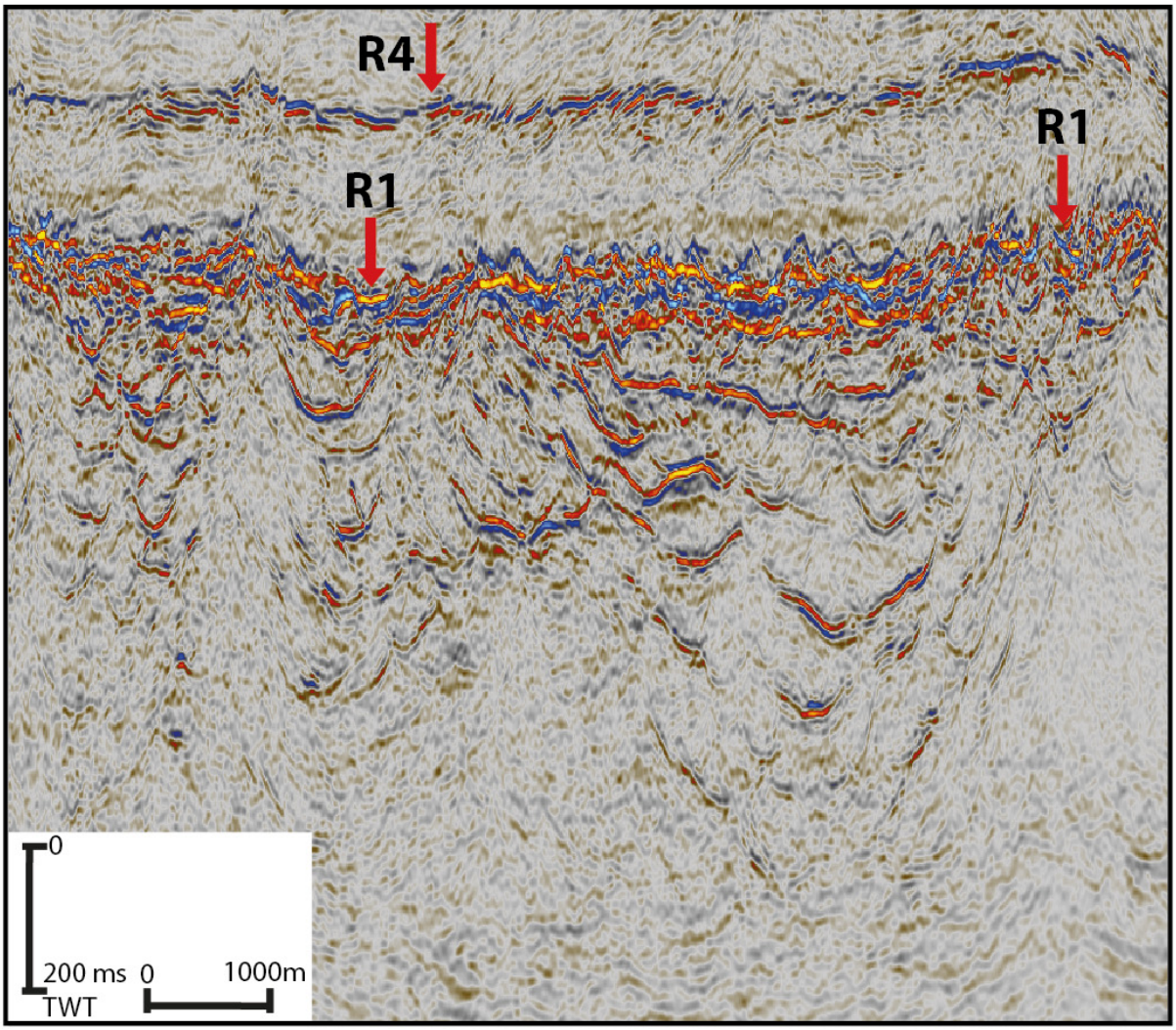

Figure 24. Well-developed example of the bow-shaped reflections below R1. It is located near the eastern termination of R1 towards the western slope of the JMR. The R4 mineral transition is visible above. R1 is located at 3500 ms TWT.

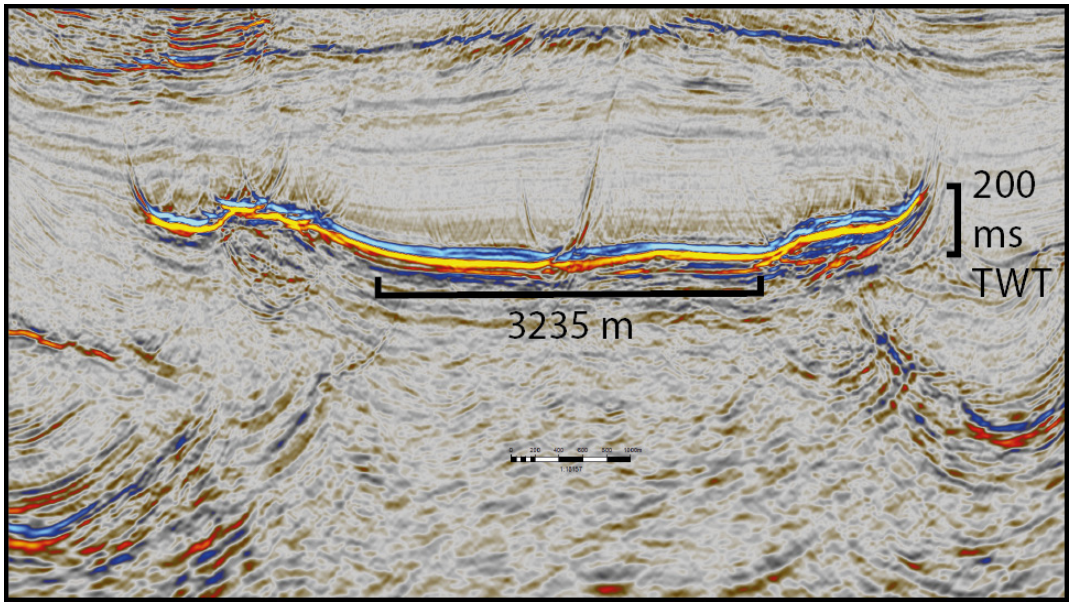

Figure 25. Reflection interpreted as a saucer-shaped intrusion in the northern part of the JMB which is not covered by R1.

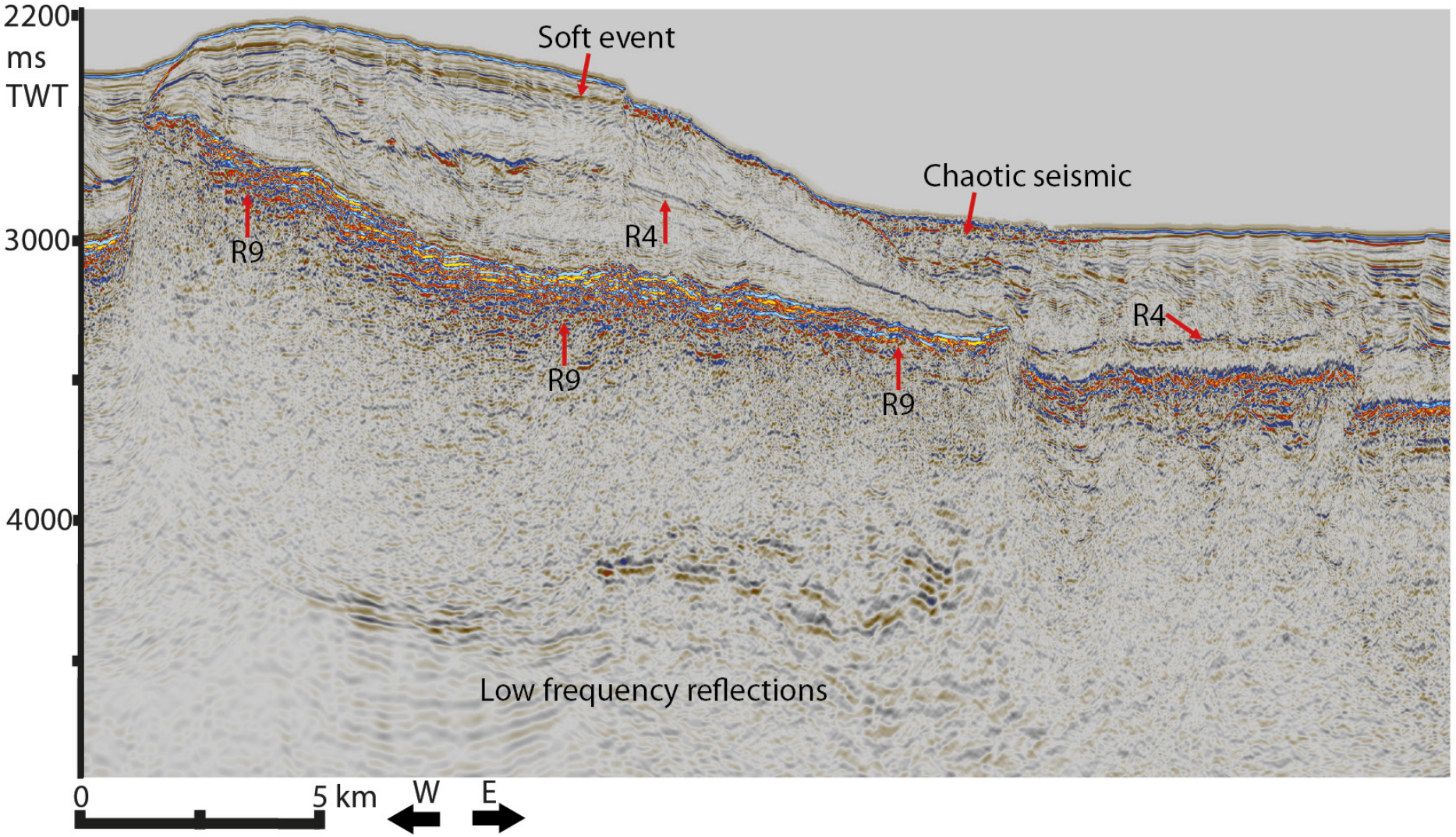

Figure 26. Observations in seismic line 4. Important features are the R1 and R9 events, the low amplitude reflections below R9, and the varying interval thickness above R1 and R9.

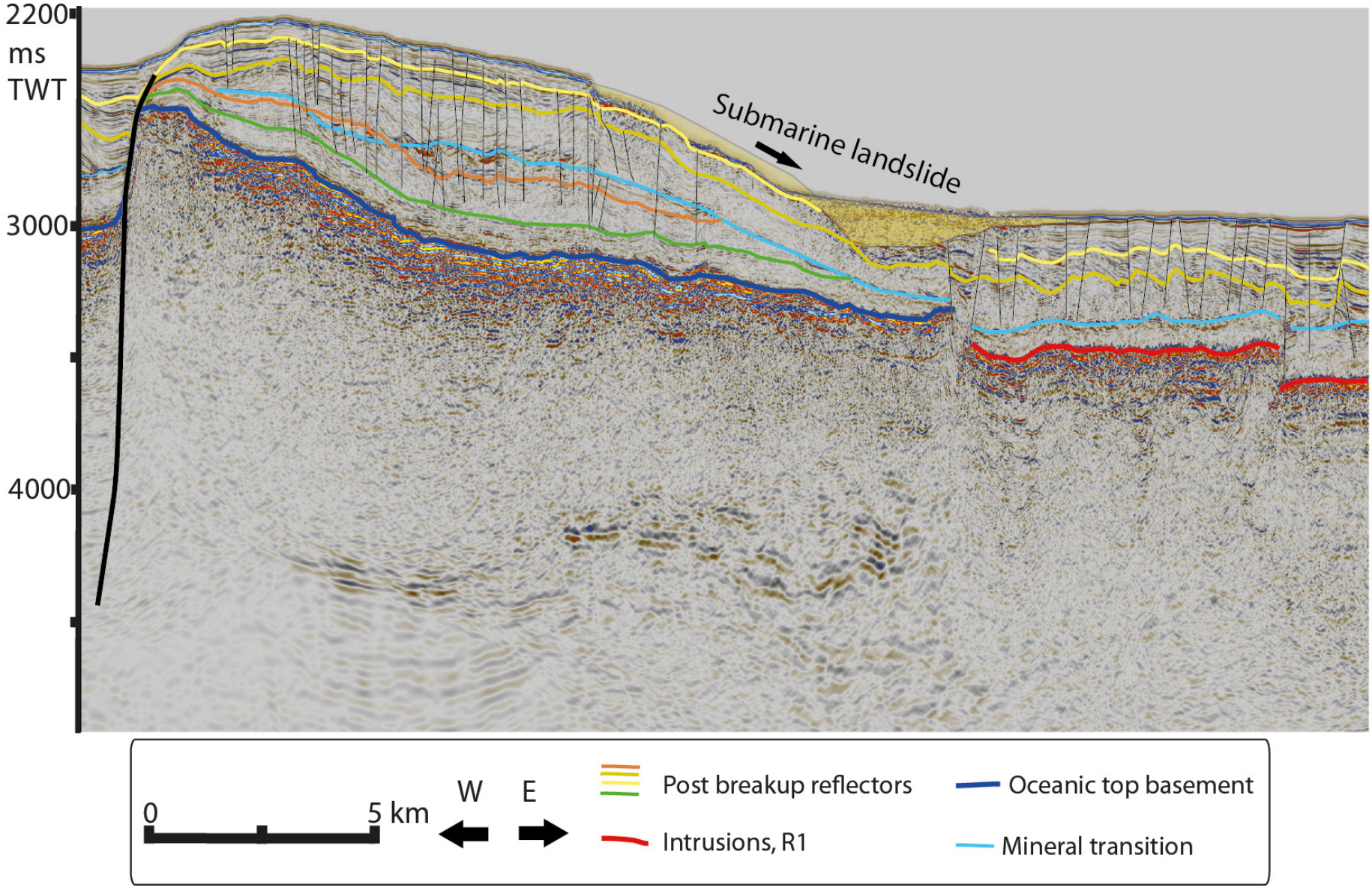

Figure 27. Interpretation of seismic line 4. R9 is interpreted as top oceanic basement, R1 as an intrusion, and a submarine landslide is visible near the sea bottom.

The eastern volcanic province

There are three main volcanic units observed on the eastern margin of the JMMC. The seaward dipping reflectors are related to the Early Eocene breaking, as is the oceanic crust. The eastern intrusions must be generated at a later stage, as they have intruded into sediments emplaced on top of the SDR and oceanic basement. They were all mapped on multiple seismic 2D lines, and the result may be viewed in Figure 29.

The SDRs were mapped along the eastern margin, using the available seismic data. They are identified as steeply easterly dipping reflections below the R3 reflector. The clarity of the reflections is varying from seismic line to seismic line, and some of the lines, such as seismic line 1 and 3, stand out with better images than the other lines. The area to the east of the Jan Mayen Trough (JMT) is not well covered by seismic data, and is therefore an uncertain area with regards to the presence of the SDRs as well as the other volcanic units. Due to the low reflectivity of the seismic below the R3 reflector determining the depth limitations of the sequence is difficult. It is also hard to interpret where the SDRs terminate towards the east, as the volcanic intrusions further mask the seismic, making it very hard to do any reliable observations.

The oceanic crust in the east is harder to identify on the eastern margin of the JMMC than on the western margin, as it is observed to be similar to the top of the SDR-sequence, which is interpreted to be deposited on top of continental crust. Further out on the oceanic crust it becomes irregular and full of small ridges, as is typical for the oceanic crust, thus discrimination is possible there. A method for discriminating between the two closer to the COB based only on seismic reflection data has not been found. From the magnetic data used in Peron-Pinvidic et al. (2012a) it is indicated that the transition to oceanic crust takes place below the intrusions or at the eastern termination of the intrusions.

The intrusions in the area are observed above and to the east of the SDR-sequence, being present along most of the margin. Interpreting exactly when the intrusions were deposited in the areas where they are constrained to the lower post breaking sediments is difficult. But north-east on the margin they are observed to intrude into the sedimentary rocks that are thought to be from the post rifting period of the second breaking (see Figure 28). It should be noted that those intrusions are different in appearance from the general trending type of intrusions seen along the margin, and that more uncertainty is involved in their interpretation as volcanic intrusions than elsewhere. The upper image in Figure 28 is a more certain interpretation, and it is deposited late in the syn-rift interval. It therefore seems likely that at least some of the intrusions were deposited at a late stage in the development of the micro continent.

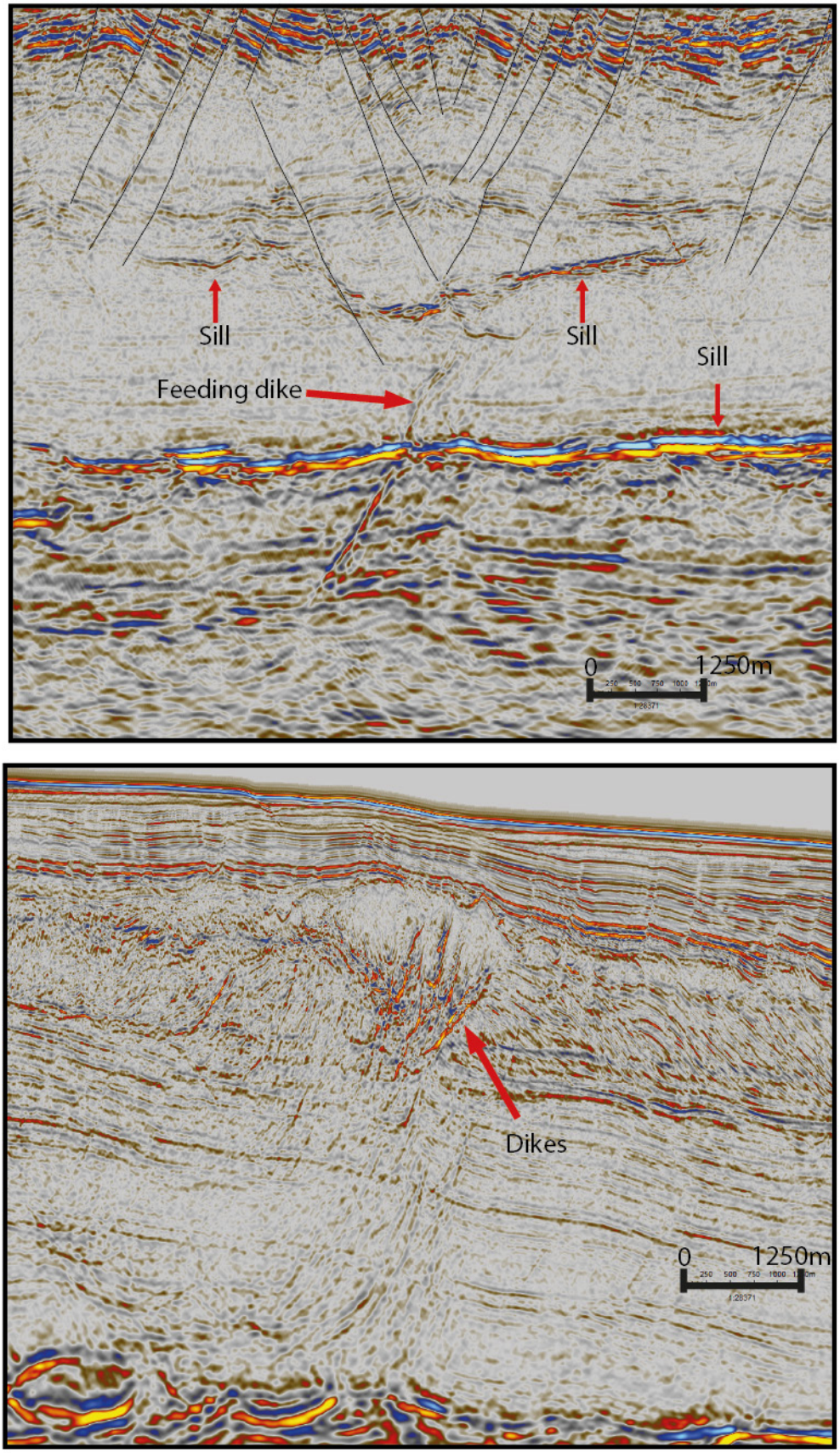

Figure 28. Interpreted intrusions on the eastern margin. Notice the feeding dike in the upper image. In the lower image, the interpreted intrusions are deposited within a post-rifting sequence of sediments.

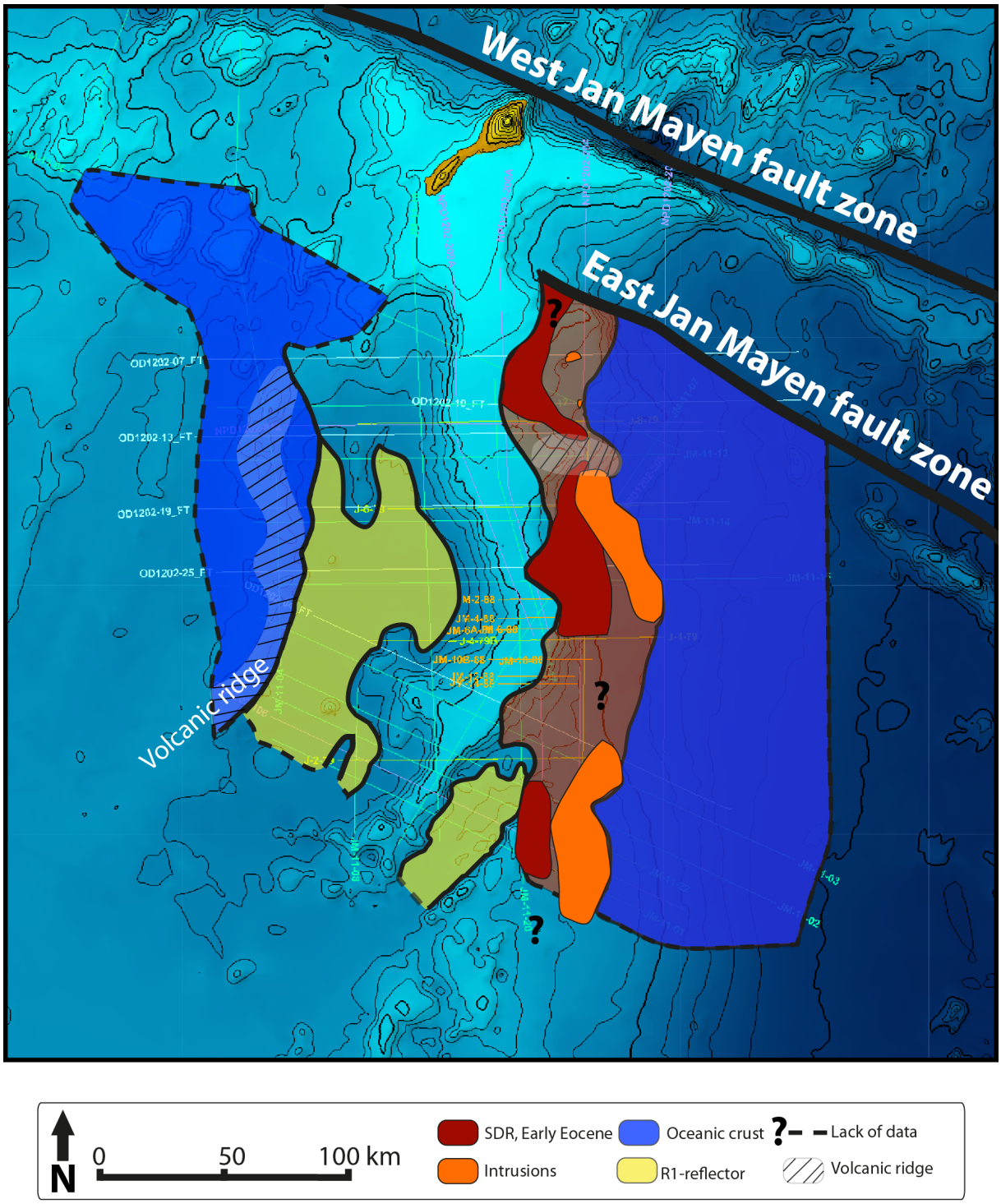

Figure 29. Surface interpretations of the volcanic reflectors in the study area on a bathymetry map. A dashed line indicates that the interpretation is uncertain due to lack of data. The blue oceanic crust is assumed to continue in both easterly and westerly directions from the interpreted area. The interpretation of oceanic crust in the east is approximate, and loosely based on the work done by Peron-Pinvidic et al. (2012a). The interpolation between the seismic lines is done manually.

Identifying volcanic facies on the eastern margin

Observations from seismic line 5

Along most of the eastern margin, the intrusions effectively masks the underlying sequence, making interpretation of any seismic facies below difficult. On the northernmost part of the margin intrusions are sparse, which should make it possible to observe changes below the R3 reflector. The most prominent features were found on seismic line 5, which may be observed in Figure 30.

The observations are concentrating on the interval below the R3 reflector. The western end of the line, some weak reflectors may be seen below the R3 reflector. The reflections appear to dip slightly steeper than the R3 reflector. As the slope gentles, the reflections terminate, and the seismic below R3 is characterized by a chaotic reflections. The dips vary within the interval, and the seismic appears noisy and blanker than the laterally surrounding areas. Eastwards of this zone, the seismic changes into higher amplitudes that dips seawards. Further east these dipping sequences are no longer seen and the reflectors appear horizontal.

Interpretation of seismic line 5

The different segments observed in seismic line 5 was interpreted as seismic facies such as described Planke et al. (2000). No landwards flows have been found, but as seen in Figure 31, an inner SDR sequence was found, as well as an outer high and an outer SDR. The outer high was identified based on its location relative to the inner SDR, together with the fact that it consists of seismic data which is significantly more chaotic than the SDR. This chaotic appearance could be a result of the explosive nature of the shallow marine volcanism that is believed to form the outer highs. The fact that the interpreted high does not represent a significant high in the topography could be a result of erosion during its creation, or simply that the volcanism never managed generate a mound due to too low production of volcanic material.

The outer SDR is interpreted based on its location seaward of the outer high, and because of its dip in the seawards direction. The transition to horizontal reflections east of the outer SDR is interpreted to represent a transition to regular oceanic crust.

This interpretation can only be made at a few lines at the northern part of the eastern margin, and does therefore represent a significant uncertainty. It should however be noted that this could be due to the fact that the eastern intrusions are less abundant in this area than further south. As the intrusions seem to effectively mask the seismic data below, it is possible that they hide the outer high and possibly also an outer SDR from the seismic.

When viewing this it should be noted that the interpretation was more model-based than the other interpretation work that has been done. This leads to a less objective interpretation, as it is “easy” to find features in the data if you are looking for them specifically, rather than creating models based on the observations one makes.

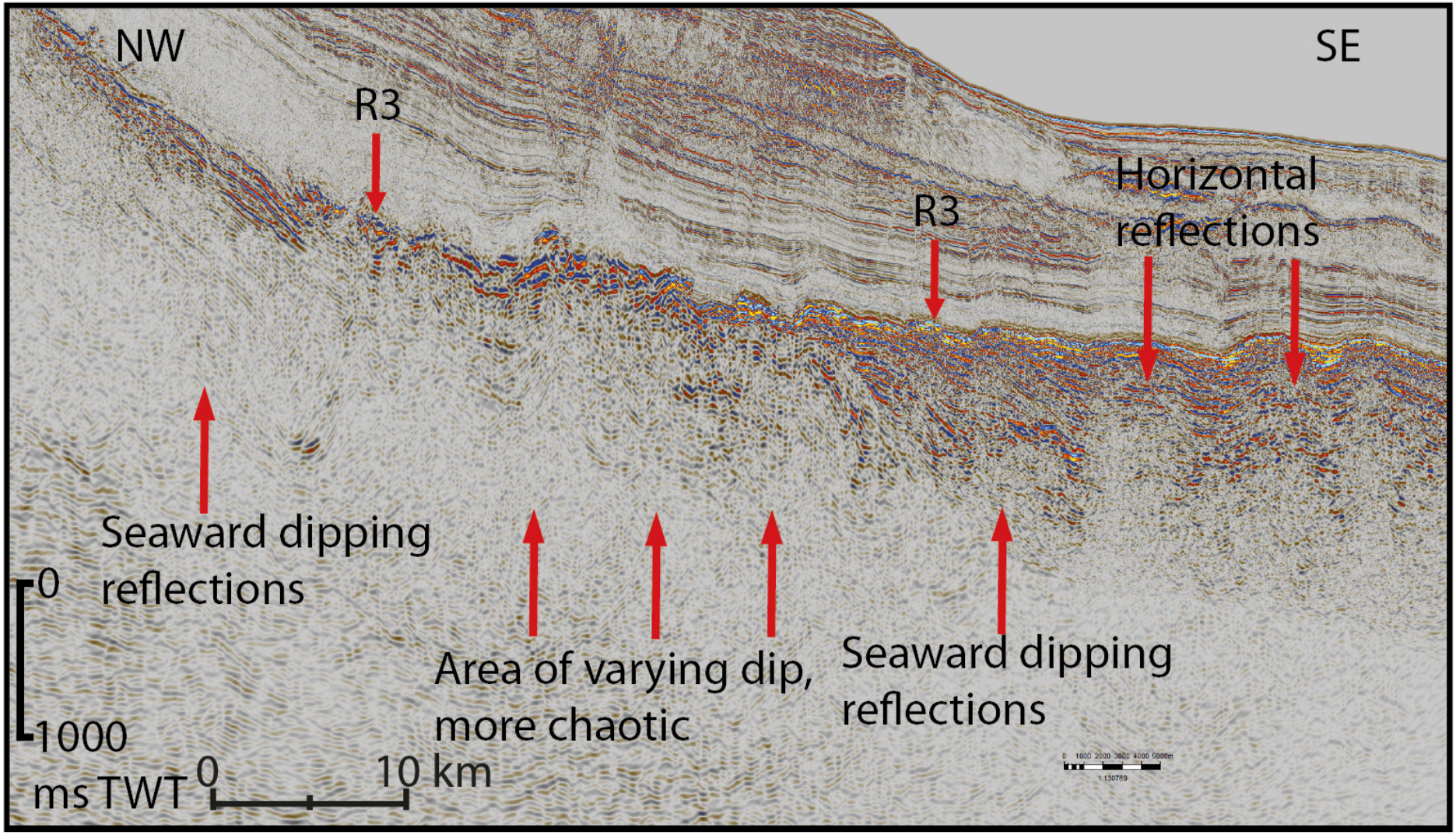

Figure 30. Observations of the volcanic facies in seismic line 5. Note the changing dip direction, and seismic appearance of the reflections below R3. The line is from NW to SE, and therefore not directly perpendicular to the JMR. The line is also quite compressed, giving unnaturally steep dips.

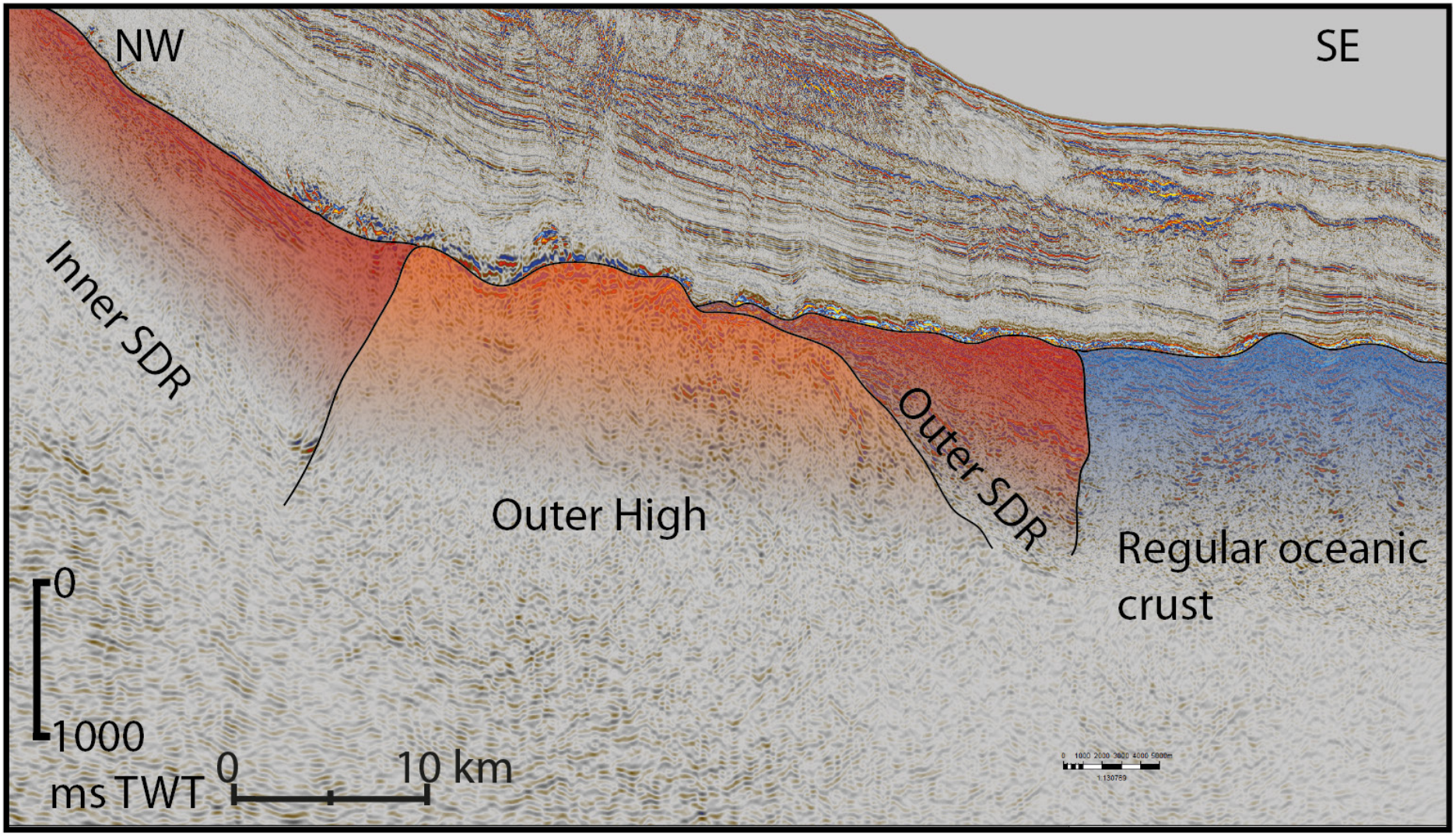

Figure 31. A volcanic facies interpretation of seismic line 5. The interpretations is based on the dip and seismic appearance of the seismic, together with the seismic volcanostratigraphy presented by (Planke et al., 2000). The interpretations are somewhat uncertain, as only a few seismic lines in the data can be interpreted in this fashion.

Interpretation of the deep reflectors

Throughout the northern part of the investigation area, it is common to observe deep reflectors, such as the ones seen in seismic line 1 and 2. On the JMR the reflections are seldom continues over longer distances, but rather appear in segments one the east and west slope, and on the top of the ridge. They seem to follow the trend of the overlying layers. They are not believed to be sea-bed multiples.
Only in the case of seismic line 1 is it possible to observe a deep reflector in the Norwegian Basin to the east of the JMR.

Due to their large depth, and that the seismic signature of the interval above and below it is interpreted that these reflectors are intra-basement. In Kodaira et al. (1998b) they use ocean bottom seismometer to create a profile displaying velocity layers in the crust on Jan Mayen, see Figure 33. Peron-Pinvidic et al. (2012a) presented a modeling of a seismic line from the micro continent based on gravity and magnetic potential field measurements, see Figure 32. Based on the similarity to these models, it is suggested that the reflections are from the boundary between the upper and lower crust.
As for the deep reflector in the Norwegian Basin the interpretation is more ambiguous. It could be the lower boundary between the outer high, and the attenuated mantle below, indicated in Figure 32. This interpretation would fit with the observation that the reflector seems to weaken and possibly disappear towards the west and east. At the same time, the distance covered by the reflector in seismic line 1 seems too long for an outer high.
It could also be the Moho-transition between the oceanic crust and the mantle or some internal velocity change within the oceanic crust.

These interpretations remain uncertain.

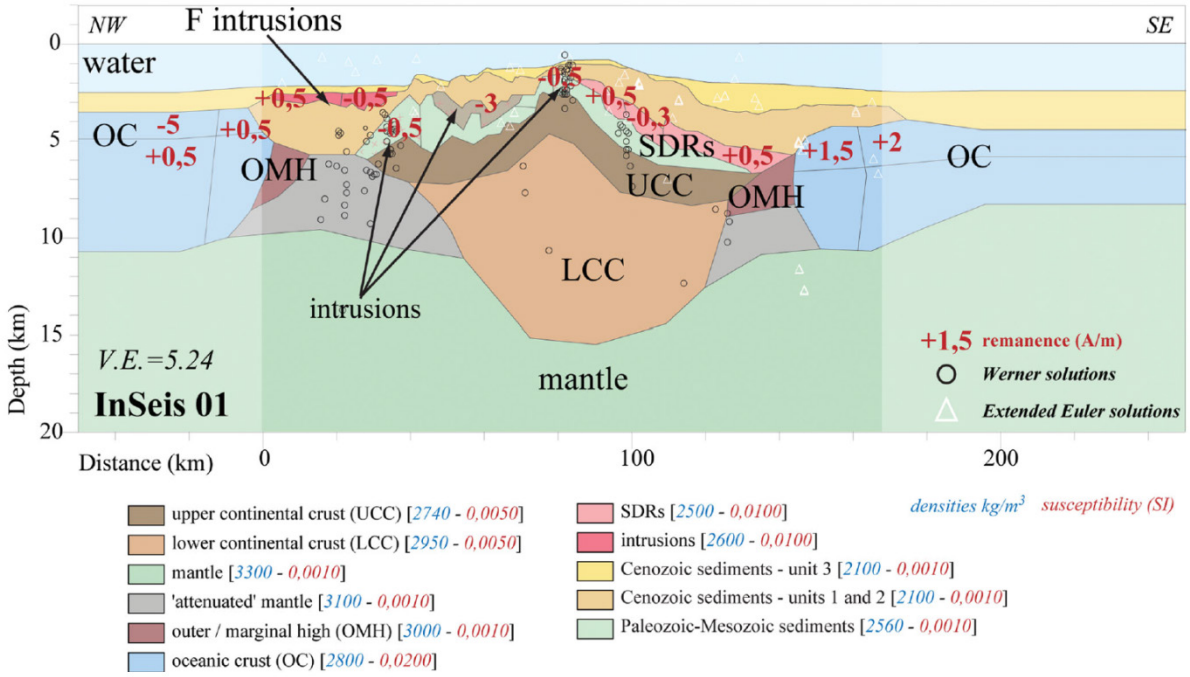

Figure 32. Model of a profile through the JMMC based on magnetic and gravimetric data. Peron-Pinvidic et al. (2012a)

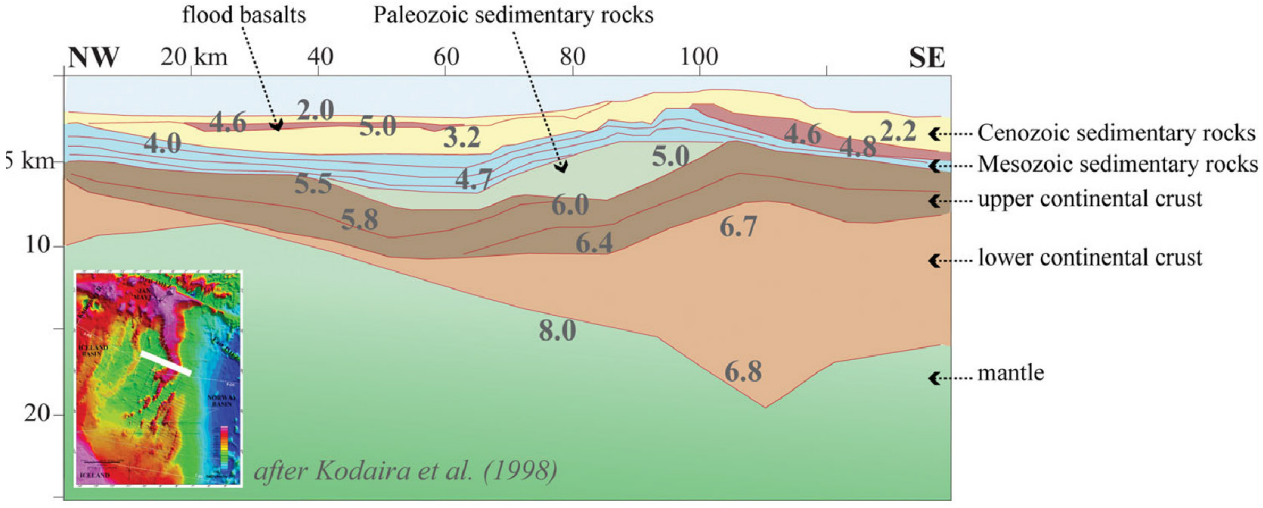

Figure 33. Seismic refraction profile from Kodaira et al. (1998b), as modified by Peron-Pinvidic et al. (2012a).

Discussion of findings

Thoughts on the intrusions in the study area.

Based on the interpretation, intrusions are abundant over the JMMC. R1 in the Jan Mayen Basin (JMB) and the Jan Mayen Trough (JMT) may be interpreted as a major intrusion in the west, emplaced after the Early Miocene breaking and the initiation of the Kolbeinsey Ridge took place. The intrusions on the eastern margin are harder to date, but some examples have been observed in the upper sedimentary sequence that is assumed to have been deposited after the main rifting episode in the west. It is therefore possible that both events have taken place at around the same time and that they are linked to the same process.
The JMB area was found to be thinned to an extreme extent, possibly down to 3 km, by the ocean bottom seismic surveys analyzed by Kodaira et al. (1998b). Such close proximity to the upper mantle could cause the area to be a zone of weakness, allowing melt from the mantle to travel up through the sedimentary rocks within the basin, creating dikes and sills. When the magma pressure reached a point where it no longer had the needed pressure to propagate further upwards, it spread out horizontally instead cross-cutting the stratigraphy. When the intrusion reached the slopes of the ridges the pressure was not sufficient to overcome the increased compressional forces, and the propagation of the intrusion stopped. The vertical shifts could be caused by zones of weakness where the intrusion was able to propagate further up, or by later fault activity.
Alternately, the sills and dikes in the basin reached all the way to the surface, and spread as submarine basalt flows, possibly sources from multiple points. No such points of eruption have been identified in the data, but could be present in between the seismic lines or outside the data set. The vertical shifts could be a result of fault activity after the deposition of the basalts. The basalt floods would stop when meeting highs in the topography.

The eastern intrusions all take place along the continent-ocean boundary, suggesting that there is a connection between the two. It can be speculated that the mantle is higher in this area as a result of the earlier sea-floor spreading. It also seems plausible that the transition between continental rock types to oceanic crust is weak, being a possible conduit area for melt from the upper mantle.

As mentioned in the chapter about the volcanism during the breaks, Mjelde et al. (2008b) and Kodaira et al. (1998b) found that the initial crust produced at the western margin was unusually thin, around 5 km, suggesting low temperatures in the upper mantle. Whether this was caused by crustal convection (Kodaira et al., 1998b) or pulsations of the temperature in the Icelandic mantle plume (Mjelde et al., 2008b) or by other causes, is unknown. What can be observed by the ocean bottom seismic in their papers is that the melt production increased after around two million years, and an unusually thick oceanic crust was created. Both papers interpret this to be a result of interaction with a mantle plume.

As a result of the timing of the intrusion events observed in this study, it is suggested that these could be a result of increased influence of the mantle plume below the JMMC. R1s

position in the stratigraphy above the oceanic top basement suggests that it was emplaced after the initiation of the sea floor spreading, possibly correlating with the time of increased oceanic crust generation. No stratigraphic correlation between these events has been investigated, and it is therefore purely speculative.
The suggested correlation would imply that the increased temperature in the mantle generated melt, which traveled up through the weakest parts of the crust; the thin JMB in the west, and the COB in the east.
An implication of significant volcanic activity in the JMB is that the basin is that the sedimentary rocks in the basin would be frequently pierced by volcanic intrusions, which would complicate and increase cost of any future hydrocarbon exploration in the area, as well as further adding complexity to the imaging process of the sedimentary rocks below R1.

The first breaking

Considering the volcanic facies that were identified along the eastern margin of the JMMC, it is found that it is a result of a volcanic continental break. Whether or not the outer high and outer SDR which were interpreted in seismic line 5 are present along all of the margin is uncertain, mainly due to the volcanic intrusions that mask the area where they would be likely to find.

The interpretation of a volcanic margin corresponds with the findings of previous studies.

The second breaking

No volcanic facies such as SDRs or outer highs were identified around the western oceanic crust. This fits the model of a non-volcanic passive margin. It should also be noted that due to the extreme thinning associated with the rifting process, the area was likely very low topographically. No significant unconformities was interpreted at the same stratigraphic level as the sea floor spreading, and it therefore seems likely to assume that the sea floor spreading happened below sea level. The lack of any chaotic high areas along the oceanic crust indicates that no shallow marine explosive volcanism took place, implying that the sea floor spreading was initiated in a deep marine environment.

This, combined with the notion of low melt production would explain the lack of volcanic facies found at the western continental margin of the JMMC.

Geological history of the JMMC

From the data interpreted in this thesis it has been attempted to reconstruct the geological history of the JMB. The history is divided into multiple stages, based on the interpretation of the volcanic sequences in the first breaking, the sedimentary sequences and their major unconformities, the uplift and subsidence with accompanied fault activity, and the interpretation of late intrusions after the second break up. Figures were drawn in order to visualize the development, but these are purely schematic and not to scale. The main input from the seismic data was provided by seismic line 1 which gave an overview of the JMR ridge, seismic line 2 which gave an overview of the development in the JMB area and seismic line 5 which included the volcanic facies. The yellow, green and orange sequences correspond to the sedimentary sequences interpreted in the seismic lines.

Stage 1; pre break rifting

Before the breakup there was significant rifting and extension between Greenland and the Eurasian plate. There was also likely some uplift due to the upwelling of the hot mantle below.

Stage 2; Initiation of volcanism

Volcanism along the breaking axis started, creating sub-aerial basalt floods towards both Greenland in the west and Eurasia in the east. The floods filled in the topography.

Stage 3; subsidence of the basalt flows

Volcanic flows fill in the area around the breaking axis while the tectonic plates start to pull apart. The result is heavy subsidence along the axis, and the inner SDR sequences observed in the seismic data set are created. The subsidence is heavier closer to the breaking axis. The most recent flood is always deposited on a slope which dips away from the breaking center.

Stage 4; submarine breaking volcanism

Following the volcanostratigraphy of Planke et al. (2000), the spreading axis subsides below sea level. First, shallow marine outer highs are created during explosive volcanism in a shallow marine environment. As observed in the data, these never build up to form significant topographical highs, perhaps due to erosion during deposition. As the subsidence continues, the explosive volcanism is replaced by submarine basalt flow, which may form an outer SDR as interpreted in seismic line 5. The sea floor spreading has begun.

Stage 5; thermal subsidence and deposition of the orange sequence

Seafloor spreading has continued, and the JM-region undergoes thermal subsidence as the mantle below cools down. The accommodation space generated is filled in by sediments building out from the Greenlandic margin while the sea level fluctuates, generating unconformities within the sequence. The newly created oceanic crust subsides more than then the continental crust, resulting in rotation and a seaward dip of the margin. The deposited orange sequence is faulted in the process.

Stage 6; rifting and deposition of green interval

The top of the yellow sequence is eroded. Rifting starts, and causes listric faults creating the JMB. Deposition of the green interval begins, and continues throughout the rifting event. The green intervals are therefore affected by the faulting in the JMB, but not as much as the underlying orange sequence.

Stage 7; rifting causes thinning of the crust

The rifting and extension continued in the JMB, causing a significant thinning of the continental crust. Some areas stand up as ridges in the JMB. The western end of the JMB is assumed to have undergone a larger degree of thinning as this is where the breaking happened at a later stage. Due to the interpretation of dramatic faults and several ridges in the southern part of the JMMC, it is likely that the extension was even more profound there than in the north. Erosion of the green interval on the eastern slope of JMR and on the ridge itself suggests further uplift above sea level.

Stage 8; the second breaking

The rifting was eventually so severe that the break in the west initiated, and the production of oceanic crust initiated. Exactly how this process took place has not been studied in detail in this thesis. Initial crustal production was slow due to low mantle temperatures according to previous studies. The yellow post-rifting sedimentary sequence starts to be deposited as the micro continent subsides below sea level. Due to the amount of rifting that probably took place, it is assumed that the initial sea-floor spreading happened below sea level.

Stage 9; intrusions, todays configuration

In the final stage, the yellow sediment package has continued deposition. A temperature increase in the mantle leads to increased melt production, which causes increased thickness of the produced oceanic crust and volcanic intrusions into the JMB and in the zone of weakness in the continent-ocean transitional area on the eastern margin. An uplift of the oceanic crust close to the ocean-continent transition is seen on the western margin.

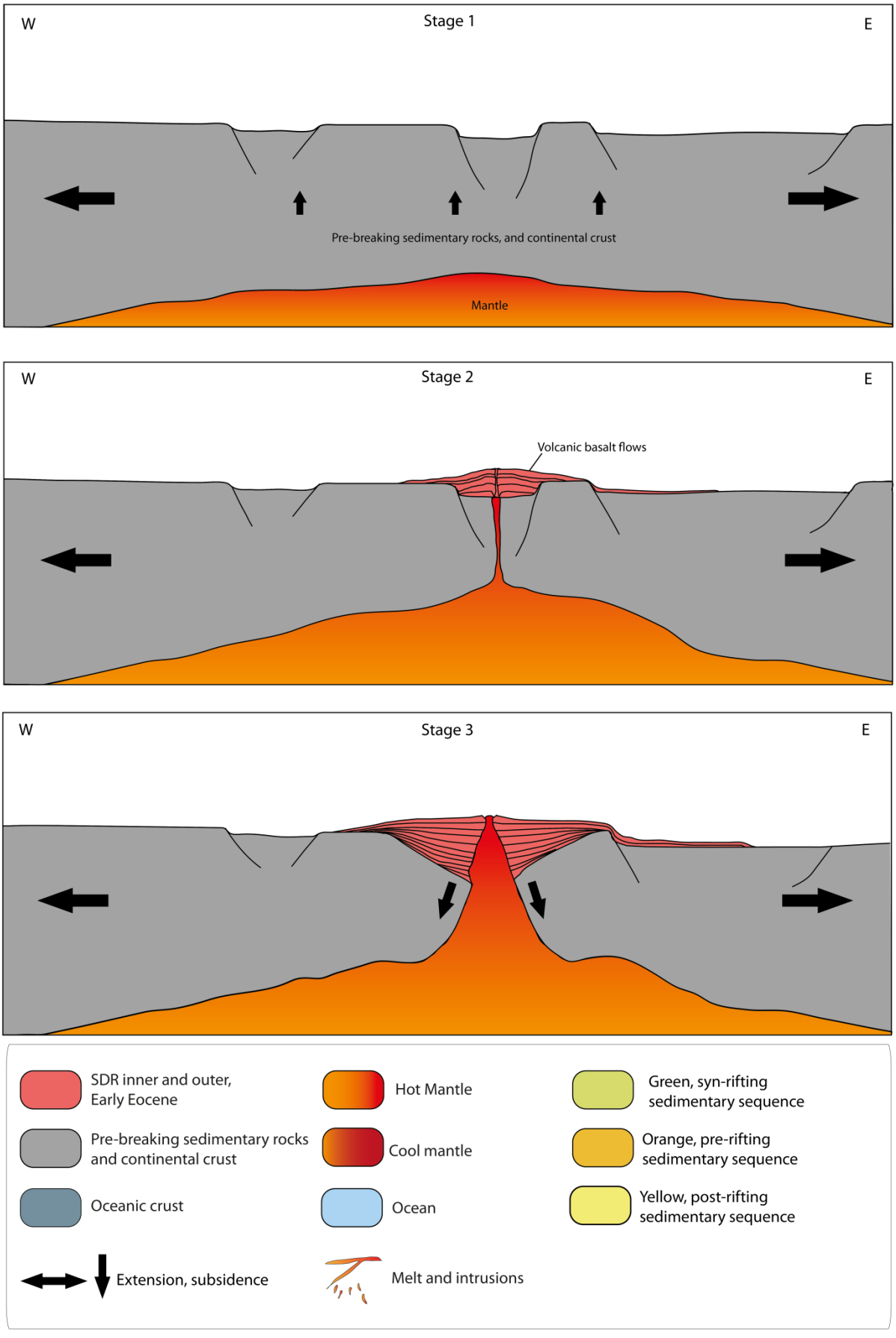

Figure 34. First three stages of the geological history. Illustrates the first breakup and the creation of the inner SDR sequence. Arrows indicate extension and subsidence.

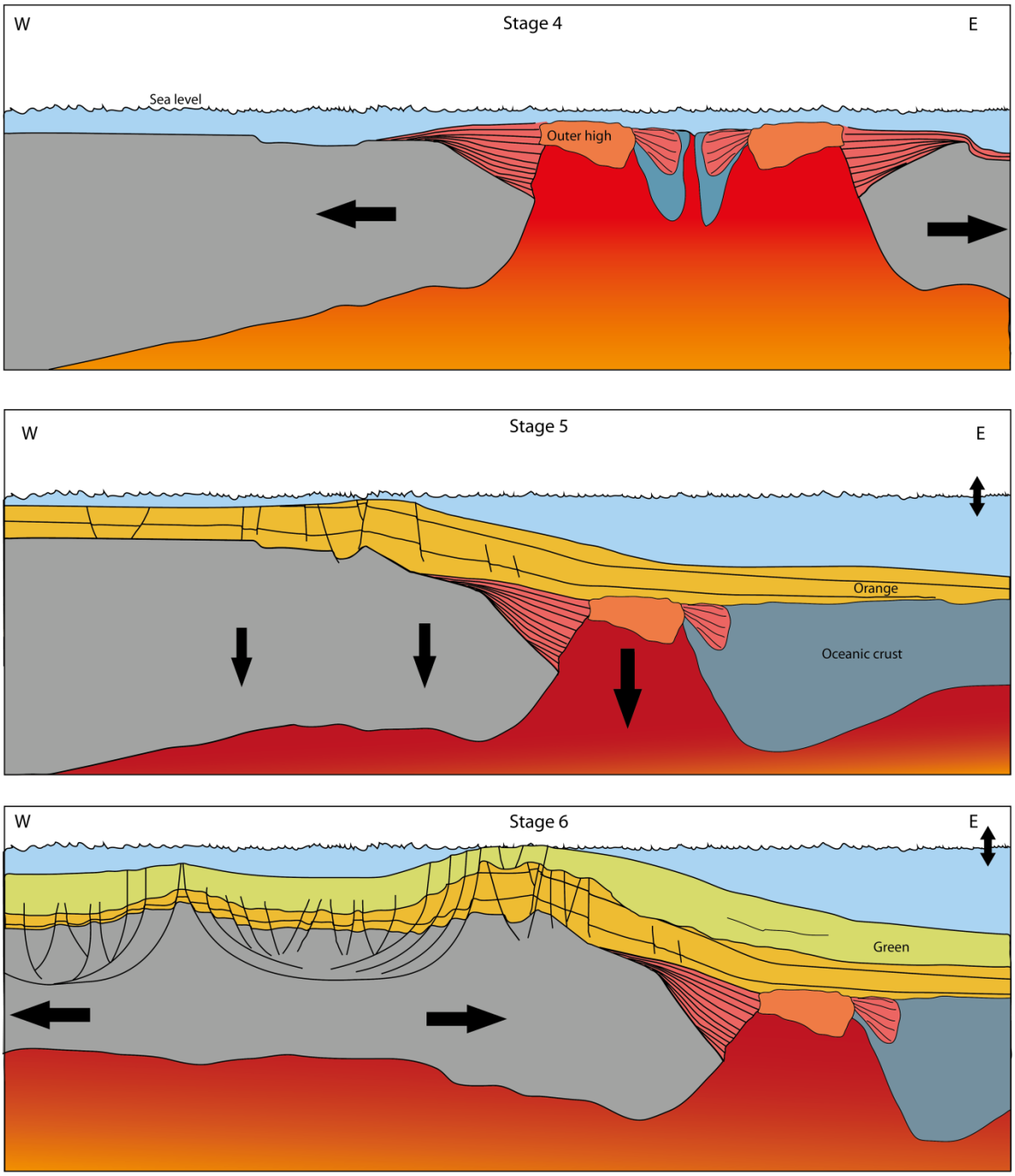

Figure 35. 4th, 5th and 6th stages of the geological history. Further illustrates volcanic facies from the first breakup, generation of oceanic crust and deposition of the first sedimentary sequences. The section viewed is shifted eastwards in the 6th stage.

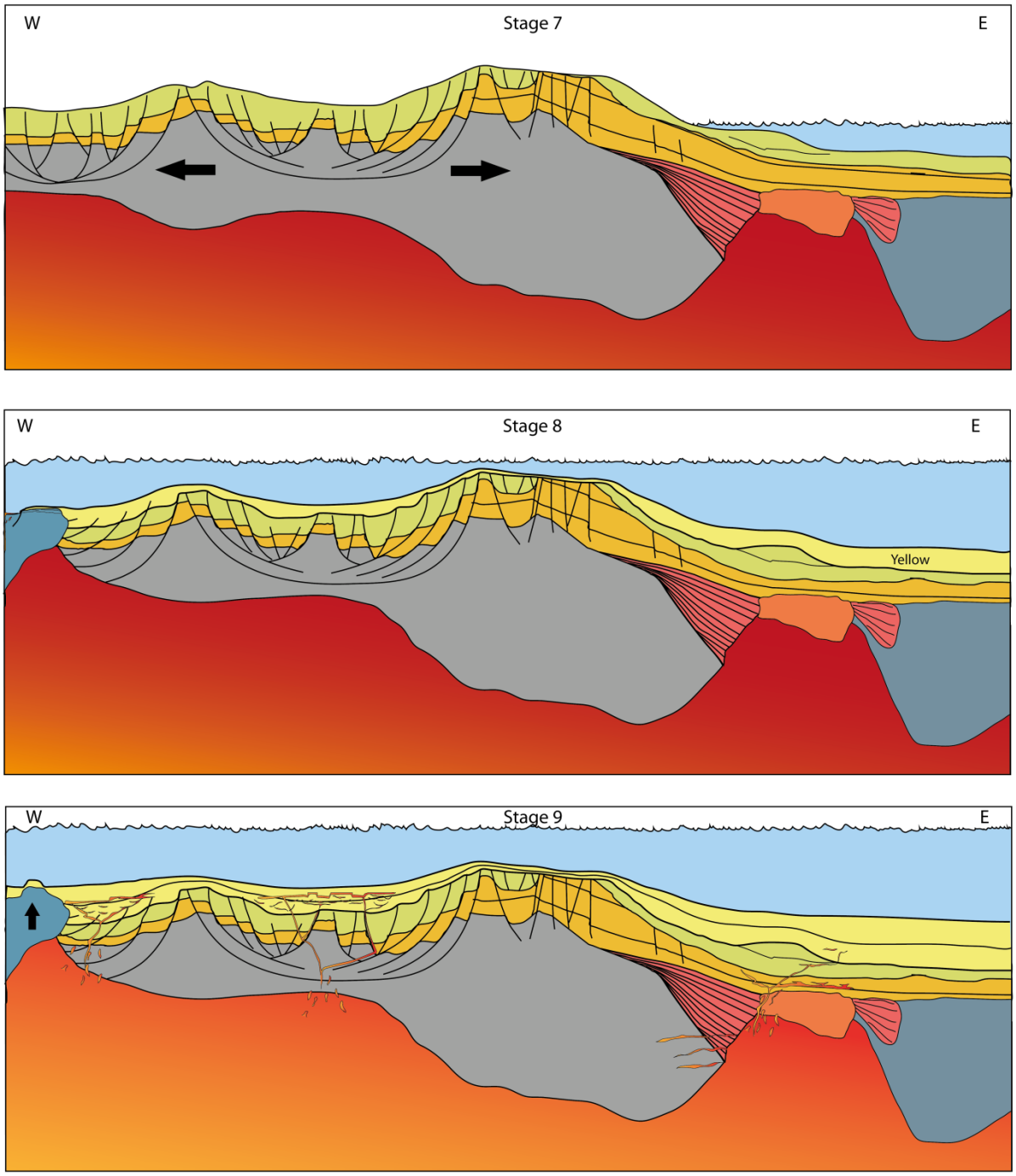

Figure 36. The final three stages of geological reconstruction. Illustrates the extreme thinning of the JMB, the start of the second breakup, deposition of the yellow sedimentary sequence and the introduction of intrusions.

Weaknesses and further work

One of the main weaknesses in this thesis that the interpretation work has mainly been done using the east-west lines in the survey. N-S trending lines have also been used to attempt correlation of interpreted surfaces, but they have not been subject to an interpretation work that is as comprehensive as the east-west trending lines.
Another feature that has not been considered to a large degree is the significant change seen between the southern and the northern lines in the investigation area.

Another feature which has not been discussed much in the thesis is the rock types and source areas for the sediments that have been deposited. Examining seismic signature for different rock types and applying those to the sediments deposited, together with a more comprehensive study of the unconformities could give more information on the paleo-sea level and the uplift and subsidence history of the micro continent.

Investigation of the volcanic facies at the conjugate Møre margin would be interesting. If outer high and outer SDRs were identified there, it would support that these facies are present at the eastern JMMC margin.
In addition, investigation of whether or not there are intrusions along the Møre COB would be interesting regarding the suggested link between the intrusions and the melt production on the JMMC. If the intrusions are present it would support the idea of the COBs as a weak zone in the crust, but at the same time it would cast doubt about the connection between intrusions and increased melt production at the JMMC. An increase in the temperature of the mantle on in the JMMC would not be expected to cause intrusions in a distant conjugate margin.

Chapter 7 Conclusion

In order to gain an understanding of the continental margins and a general understanding of the geological and structural development on the Jan Mayen micro continent, recent broadband 2D seismic data has been observed and interpreted. Major findings were identification of volcanic reflectors, sedimentary sequences and identification of oceanic crust. These were summarized in a reconstruction of the geological development on the micro continent.

In the Early Eocene, Greenland and the Eurasian plate broke apart, generating a volcanic margin on the eastern margin of the Jan Mayen area. During the sea-floor spreading on the Aegir Ridge, accumulation space in the Jan Mayen area was filled in with sediments from Greenland, before the area became subject to significant extension. Sedimentation continued throughout the extensional phase, only disrupted by erosive events that could be caused by uplift of sea-level variations. Sedimentary sequences from pre, syn and post-rifting were identified and interpreted in the seismic data. Eventually, the Aegir Ridge died out, and a non-volcanic break on the western margin of the Jan Mayen area separated the micro continent from Greenland. Previous work has shown that the initial production of melt was low, but that it increased after some time. Although the connection is speculative, it is suggested in this thesis that the increase in melt production lead to an extensive distribution of volcanic intrusions throughout the Jan Mayen Basin, as well as the area above the eastern continent-ocean transition. A large volcanic reflector that masks the seismic in the JMB and the JMT is interpreted to be a part of the intrusives. The intruded areas are thought to have been areas of weakness in the crust. The JMB is thought to be weak because of the extensive rifting which has thinned the crust, and the western margin because of a thin crust together with a transition between continental to oceanic rock types.

An important implication of this interpretation is the presence of numerous intrusions in the JMB-area, which would further complicate it as a potential area of future hydrocarbon exploration.

Chapter 8 . References

Breivik, A. J., R. Mjelde, J. I. Faleide, and Y. Murai, 2006, Rates of continental breakup magmatism and seafloor spreading in the Norway Basin–Iceland plume interaction: Journal of Geophysical Research: Solid Earth (1978–2012), v. 111.

Brekke, H., 2000, The Tectonic evolution of the Norwegian Sea Continental Margin with emphasis on the Vøring and Møre Basins: The Geological Society of London, v. 167, p. 327-378.

C. Berndt, S. P., E. Alvestad, F. Tsikalas, T. Rasmussen, 2001, Seismic volcanostratigraphy of the Norwegian Margin: constraints on tecnomagmatic break-up processes: Journal of the Geological Society, v. 158, p. 413-426.

Eldholm, O., J. Thiede, and E. Taylor, 1989, Evolution of the Vøring volcanic margin: Proceedings of the ocean drilling program, scientific results, p. 1033-1065.

Faleide, J. I., F. Tsikalas, A. J. Breivik, R. Mjelde, O. Ritzmann, O. Engen, J. Wilson, and O. Eldholm, 2008, Structure and evolution of the continental margin off Norway and the Barents Sea: Episodes, v. 31, p. 82.

Galland, O., S. Planke, E.-R. Neumann, and A. Malthe-Sørenssen, 2009, Experimental modelling of shallow magma emplacement: Application to saucer-shaped intrusions: Earth and Planetary Science Letters, v. 277, p. 373-383.

Gernigon, L., C. Gaina, O. Olesen, P. J. Ball, G. Péron-Pinvidic, and T. Yamasaki, 2012, The Norway Basin revisited: From continental breakup to spreading ridge extinction: Marine and Petroleum Geology, v. 35, p. 1-19.

Gunnarsson, K., M. Sand, and S. Gudlaugsson, 1989, Geology and hydrocarbon potential of the Jan Mayen Ridge: Norwegian Petroleum Directorate.

Kodaira, S., R. Mjelde, K. Gunnarsson, H. Shiobara, and H. Shimamura, 1998a, Evolution of oceanic crust on the Kolbeinsey Ridge, north of Iceland, over the past 22 Myr: TERRA NOVA-OXFORD-, v. 10, p. 27-31.

Kodaira, S., R. Mjelde, K. Gunnarsson, H. Shiobara, and H. Shimamura, 1998b, Structure of the Jan Mayen microcontinent and implications for its evolution: Geophysical Journal International, v. 132, p. 383-400.

Kuvaas, B. K., S, 1997, The Formation Of the Jan Mayen microcontinent: the missing piece in the continental puzzle between Møre-Vøring Basins and East Greenland: First Break, v. 15, p. 239-247.

Mjelde, R., A. J. Breivik, T. Raum, E. Mittelstaedt, G. Ito, and J. I. Faleide, 2008a, Magmatic and tectonic evolution of the North Atlantic: Journal of the Geological Society, v. 165, p. 31-42.

Mjelde, R., I. Eckhoff, S. Solbakken, S. Kodaira, H. Shimamura, K. Gunnarsson, A. Nakanishi, and H. Shiobara, 2007, Gravity and S-wave modelling across the Jan Mayen Ridge, North Atlantic; implications for crustal lithology: Marine Geophysical Researches, v. 28, p. 27-41.

Mjelde, R., T. Raum, A. J. Breivik, and J. I. Faleide, 2008b, Crustal transect across the North Atlantic: Marine Geophysical Researches, v. 29, p. 73-87.

Mutter, J. C., 1985, Seaward dipping reflectors and the continent-ocean boundary at passive continental margins: Tectonophysics, v. 114, p. 117-131.

Myhre, A. M., O. Eldholm, and E. Sundvor, 1984, The Jan May en Ridge: present status: Polar Research, v. 2, p. 47-59.

Parkin, C., and R. White, 2008, Influence of the Iceland mantle plume on oceanic crust generation in the North Atlantic: Geophysical Journal International, v. 173, p. 168-188.

Peron-Pinvidic, G., L. Gernigon, C. Gaina, and P. Ball, 2012a, Insights from the Jan Mayen system in the Norwegian-Greenland sea-I. Mapping of a microcontinent: Geophysical Journal International, v. 191, p. 385-412.

Peron-Pinvidic, G., L. Gernigon, C. Gaina, and P. Ball, 2012b, Insights from the Jan Mayen system in the Norwegian-Greenland Sea-II. Architecture of a microcontinent: Geophysical Journal International, v. 191, p. 413-435.

Péron-Pinvidic, G., and G. Manatschal, 2010, From microcontinents to extensional allochthons: witnesses of how continents rift and break apart?: Petroleum Geoscience, v. 16, p. 189-197.

Planke, S., E. Alvestad, and O. Eldholm, 1999, Seismic characteristics of basaltic extrusive and intrusive rocks: The Leading Edge, v. 18, p. 342-348.

Planke, S., P. A. Symonds, E. Alvestad, and J. Skogseid, 2000, Seismic volcanostratigraphy of large-volume basaltic extrusive complexes on rifted margins: Journal of Geophysical Research: Solid Earth (1978–2012), v. 105, p. 19335-19351.

Polteau, S., E. Ferré, S. Planke, E.-R. Neumann, and L. Chevallier, 2008a, How are saucer-shaped sills emplaced? Constraints from the Golden Valley Sill, South Africa: Journal of Geophysical Research, v. 113, p. B12104.

Polteau, S., A. Mazzini, O. Galland, S. Planke, and A. Malthe-Sørenssen, 2008b, Saucer-shaped intrusions: Occurrences, emplacement and implications: Earth and Planetary Science Letters, v. 266, p. 195-204.

Rubin, A. M., 1995, Propagation of magma-filled cracks: Annual Review of Earth and Planetary Sciences, v. 23, p. 287-336.

Saunders, A., J. Fitton, A. Kerr, M. Norry, and R. Kent, 1997, The north atlantic igneous province: Geophysical Monograph Series, v. 100, p. 45-93.

Skogseid, J., S. Planke, J. I. Faleide, T. Pedersen, O. Eldholm, and F. Neverdal, 2000, NE Atlantic continental rifting and volcanic margin formation: SPECIAL PUBLICATION-GEOLOGICAL SOCIETY OF LONDON, v. 167, p. 295-326.

Zhu, J., L. Lines, and S. Gray, 1998, Smiles and frowns in migration/velocity analysis: Geophysics, v. 63, p. 1200-1209.

Chapter 9 List of figures